Electronic Supplementary Material (ESI) for ChemComm.

Electronic Supporting Information for

Improved Access to Polythioesters by Heterobimetallic Aluminium Catalysis

Table of Contents

Section S1: General methods

Solvents and reagents were obtained from commercial sources and used as received unless stated otherwise. If "dried solvents" were used these were obtained by different procedures. THF was dried over K/benzophenone and distilled under argon, collected, and stored over pre-dried 4 Å sieves before use. Acetonitrile was dried over CaH_2 before distillation. $CDCl_3$ was dried over CaH_2 before vacuum distillation, degassed and stored over 4 Å in the glove box. CHO and vCHO were dried over calcium hydride at room temperature for 3 days, vacuum distilled, degassed, and stored inside an argon filled glovebox prior to use. CO_2 Grade 5.3 (Linde) was used for all polymerization studies and dried through a VICI purifier columns prior to use. The ligands $\mathbf{L^{Cy}}H_2$, $\mathbf{L^{Ph}}H_2$, $\mathbf{L^{en}}H_2$ and $\mathbf{L^{pro}}H_2$ as well as phthalic thioanhydride (PTA) were synthesised according to the literature.[1]

NMR spectra were recorded by using a Jeol JNMECA 400II, Bruker Advance 600 and 700 MHz spectrometer. ^1H and $^{13}C\{^1H\}$ chemical shifts are referenced to the residual proton resonance of the deuterated solvents. Elemental analysis was collected on a Vario EL instrument. High-resolution ESI mass spectra were obtained using a Waters UPLC-Synapt G2-S HDMS. Infrared spectra were measured using a Thermo-Nicolet Nexus 670 FTIR spectrometer with DuraSampl IR accessory in total reflection at room temperature. TGA data was measured using a Netzsch TG 209. Differential scanning calorimetry (DSC) was measured on a Netzsch 204 F1 "Phoenix" at a heating rate of 10.0 K/min. DSC thermograms are presented for the data obtained after the first heating cycle to ensure removal of the thermal history of the sample. The molecular weight and polydispersity of the polymers were determined by a Waters 515 Gel permeation chromatography (GPC) instrument equipped with two linear PLgel columns (Mixed-C) following guard column and a differential refractive index detector using tetrahydrofuran as the eluent at a flow rate of 1.0 mL/min at 30 °C and a series of narrow polystyrene standards for the calibration of the columns. Each polymer sample was dissolved in HPLC-grade THF (5 mg/mL) and filtered through a 0.20 µm porous filter frit prior to analysis.

General polymerisation protocol:

ROCOP with (thio)anhydride/epoxide:

The catalyst and the monomers were added to an oven dried vial equipped with a stirrer bar and sealed with a melamine cap containing a Teflon inlay inside an argon filled glovebox. The vial was then brought outside the glovebox and placed in a pre-heated aluminium block at the specified temperature for the specified time. At specified points of the reaction, the polymerisation mixture was cooled down to room temperature and an aliquot was removed and analysed by ^1H NMR for the determination of the conversion. At the end point, the conversion was determined again, before dissolving the mixture in 5 mL DCM and adding it dropwise to 50 mL of MeOH causing precipitation of the polymer, which was then isolated by centrifugation. This precipitation was repeated once more from DCM/pentane, and the obtained polymer was dried in a vacuum oven before further analysis.

ROTERP with CO_2:

The catalyst and the monomers were added to an oven dried Schlenk tube with a stirrer bar and sealed with a screw cap containing a Teflon inlay inside an argon filled glovebox. The tube was then pressurised with 4 bar dry CO_2 and heated at the appropriate temperature for the specified time under a constant supply of CO_2. At the end point, the reaction mixture was cooled, the excess CO_2 pressure was released, and an aliquot was taken to determine the conversion before dissolving the mixture in 5mL DCM and adding it dropwise to 50 mL of MeOH causing precipitation of the polymer, which was then isolated by centrifugation. This precipitation was repeated once more from DCM/pentane, and the obtained polymer was dried in a vacuum oven before further analysis. Reactions under 40 bar pressure were conducted analogously using a high-pressure Parr reactor.

Section S2: Adduct formation of $L^XAlM(OAc)_y$

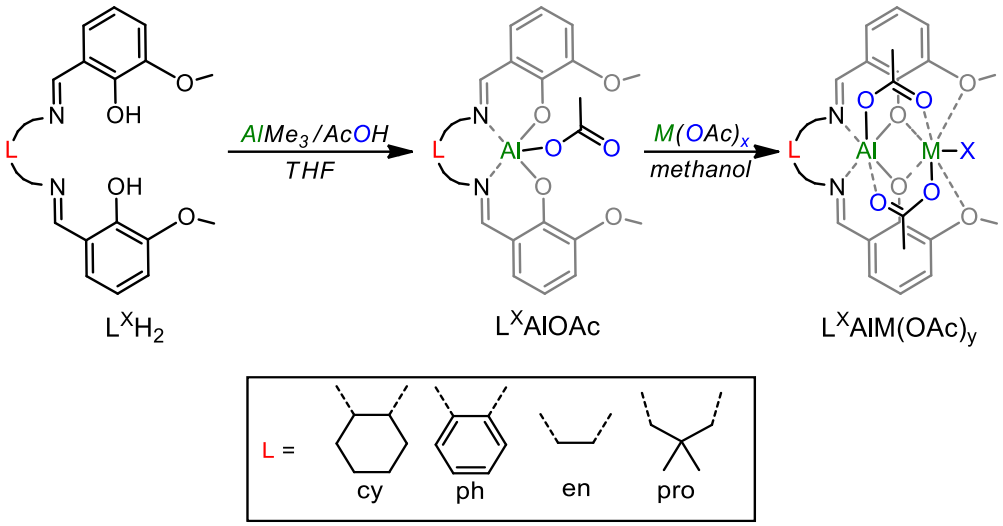

Scheme S 1: Synthesis of $L^XAlM(OAc)_y$.

The synthesis of L^XAlOAc was conducted using a modified literature preparation.[2] Under inert conditions, L^XH_2 (4.29 mmol, 1 eq.) was dissolved in 20 mL THF, 1 M $AlMe_3$ (4.29 mL, 1.1 eq.) in THF was added slowly and stirred for 2 h at room temperature. Glacial acetic acid (2 eq.) was then added and the solution was stirred for another 20 h at room temperature. The precipitate was isolated by filtration, washed with toluene (x2) and pentane, dried under vacuum to obtain a white - yellow powder. The spectroscopic data agreed with the literature. To form the metal acetate adducts L^XAlOAc (0.912 mmol, 1 eq.) was suspended with $M(OAc)_{y-1}$ (0.912 mmol, 1 eq.) in 100 mL methanol, heated briefly until reflux with a heatgun and then stirred for 1 h at room temperature. Methanol was removed under reduced pressure and the product was washed thrice with diethyl ether and dried to obtain a white powder. Yield: 80-95 %. In the case of $L^{pro}AlOAc$ the reaction had to be performed in dry acetonitrile under inert conditions. Thereafter adduct formation was confirmed by NMR spectroscopy.

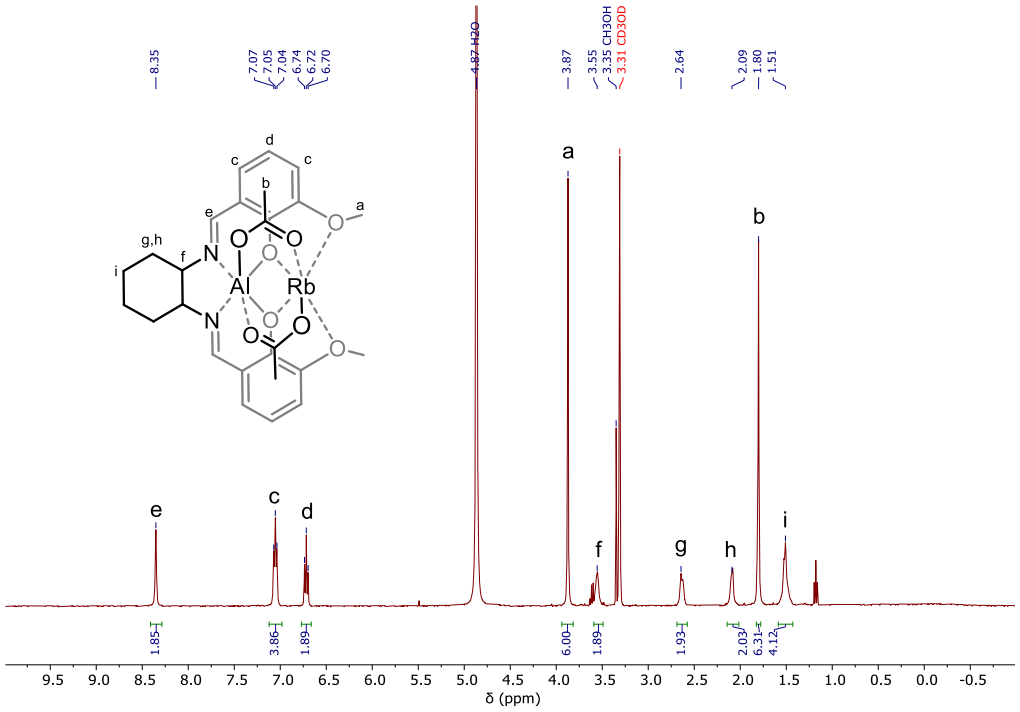

Figure S 1: ^1H NMR spectrum (400 MHz, CD_3OD) of $L^{Cy}Al(OAc)$ with RbOAc.

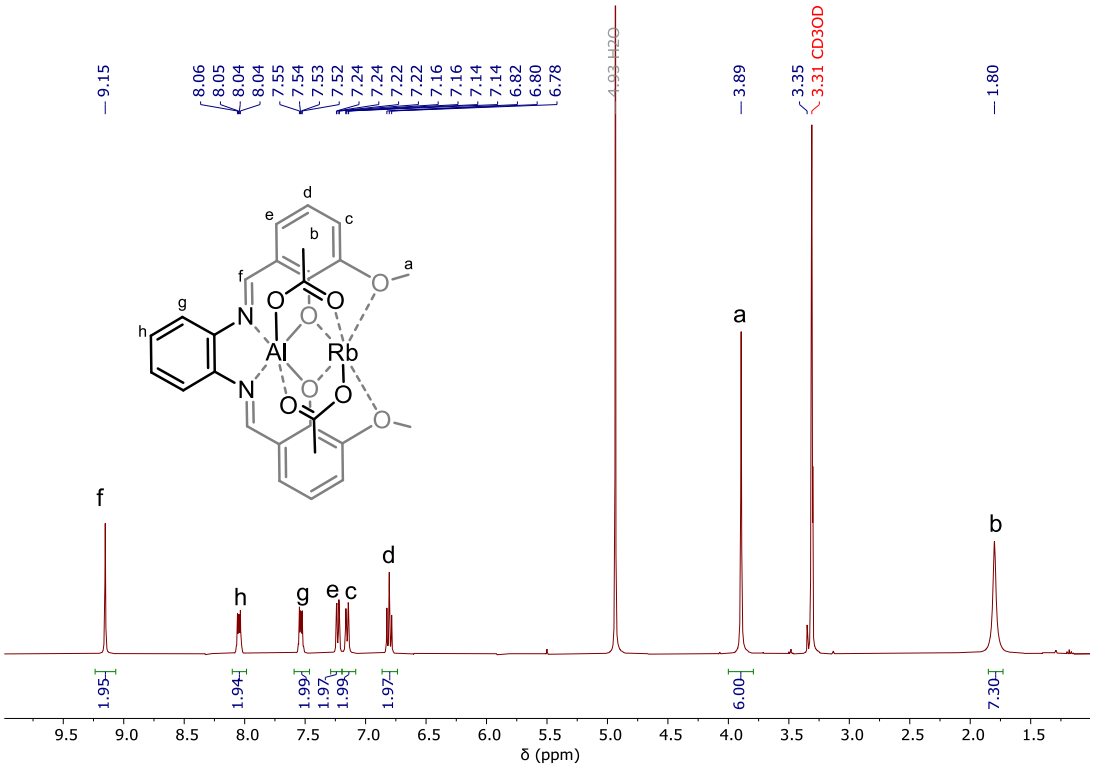

Figure S 2: ^{1}H NMR spectrum (400 MHz, CD_3OD) of $L^{Ph}Al(OAc)$ with RbOAc.

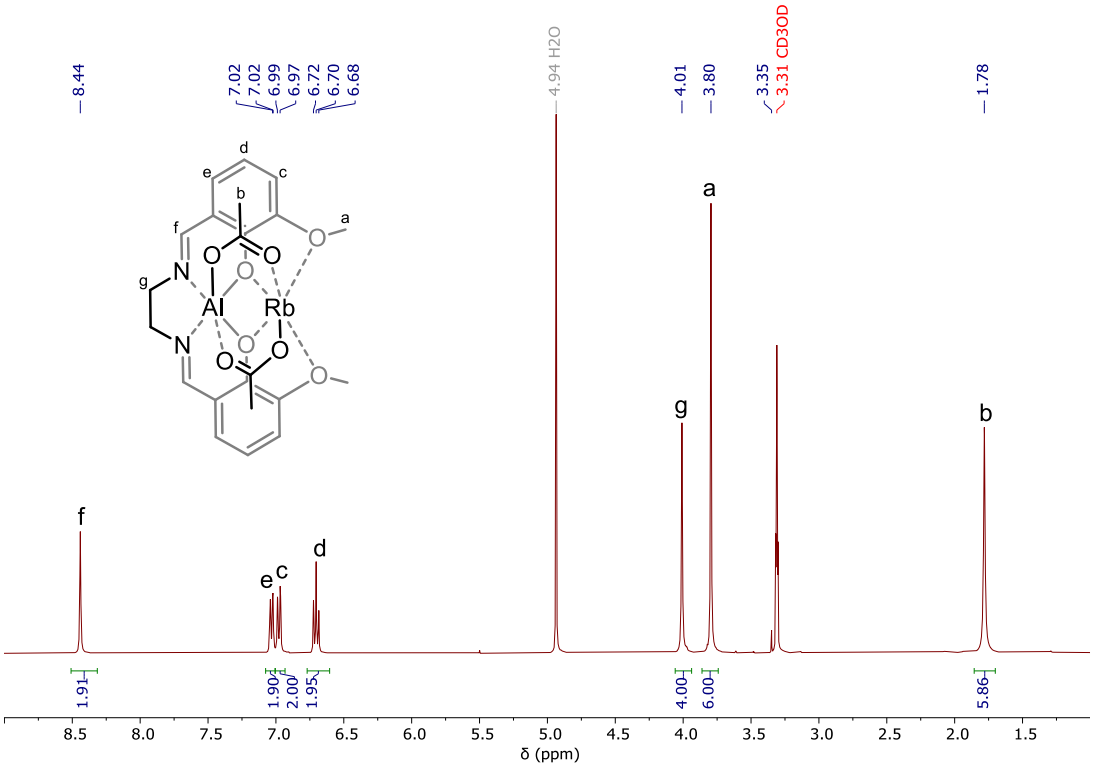

Figure S 3: ^{1}H NMR spectrum (400 MHz, CD_3OD) of $L^{en}AlOAc$ with RbOAc.

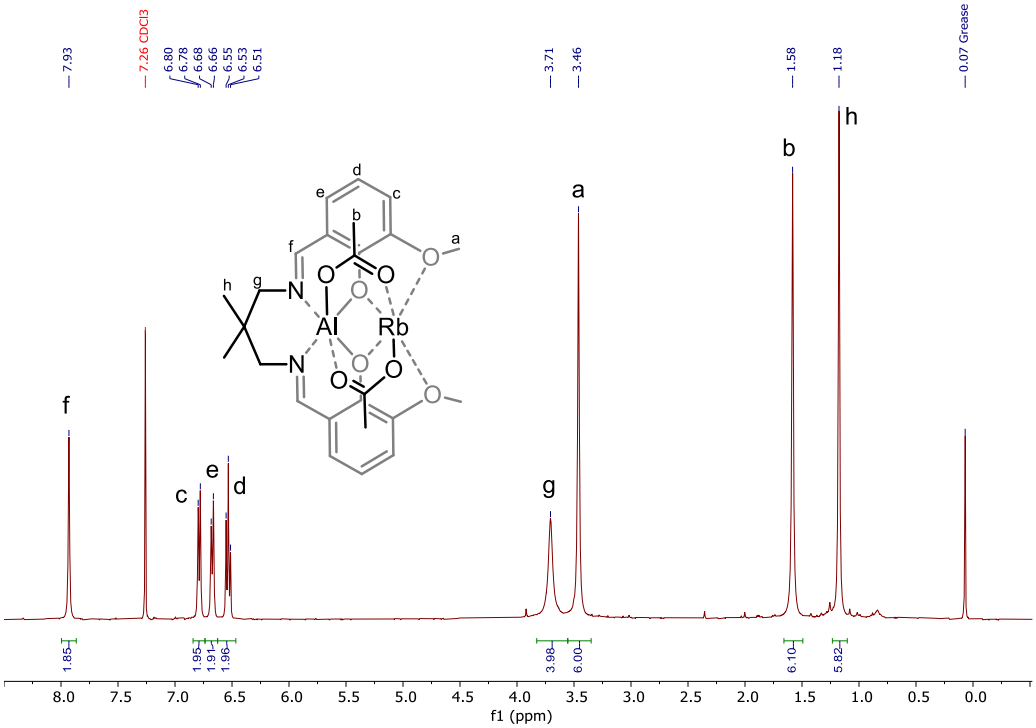

Figure S 4: ^{1}H NMR spectrum (400 MHz, $CDCl_3$) of ^{pro}LAlOAc with RbOAc.

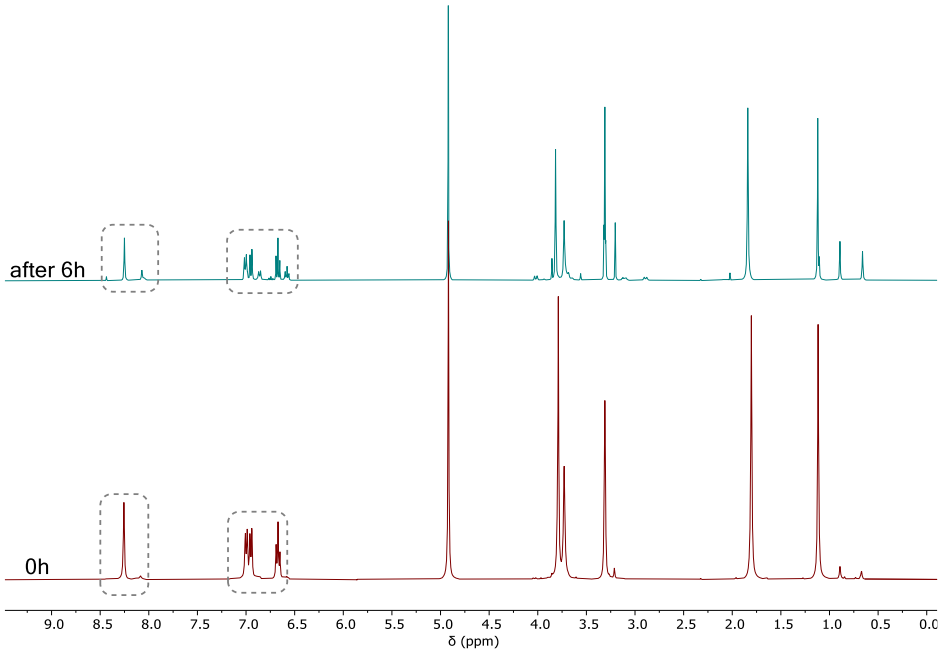

Figure S 5: Stacked ^{1}H NMR spectra (400 MHz, CD_3OD) of L^{pro}AlOAc with RbOAc showing decomposition.

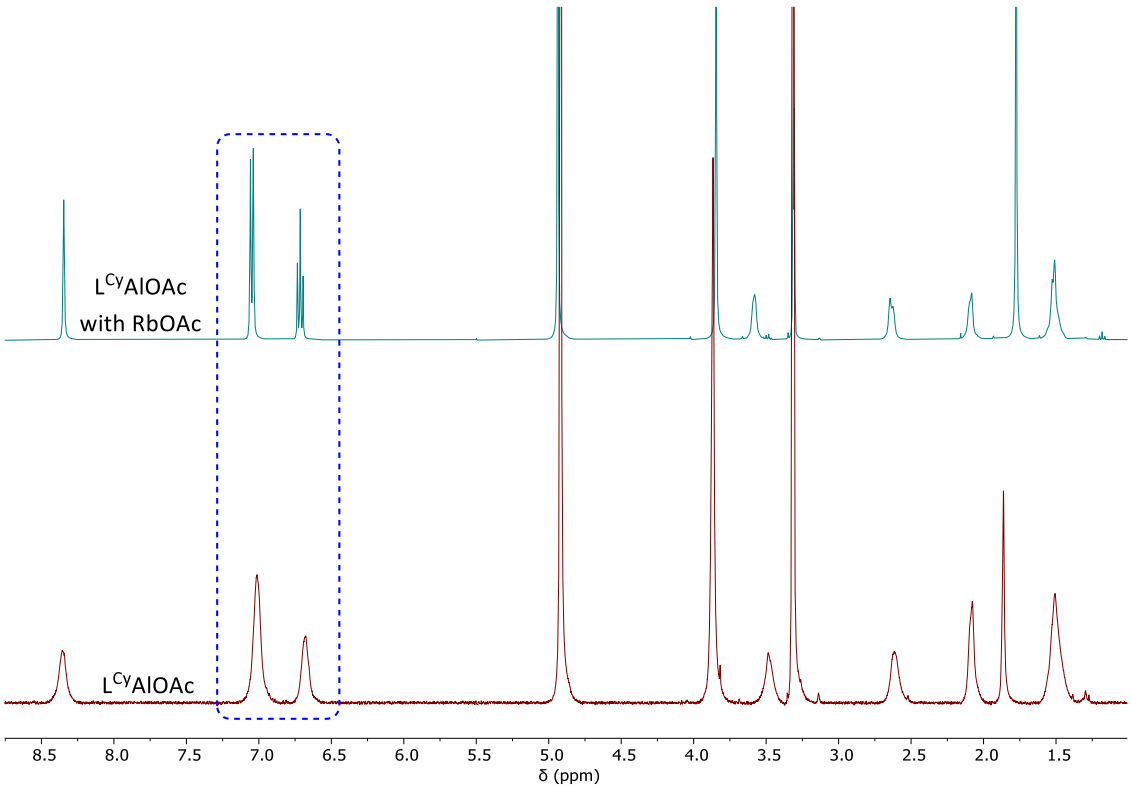

Figure S 6: Stacked ^{1}H NMR spectra (400 MHz, CD_3OD) of $L^{Cy}AlOAc$ with RbOAc and $L^{Cy}AlOAc$ showing sharper signals and slight downfield shifting indicating adduct formation.

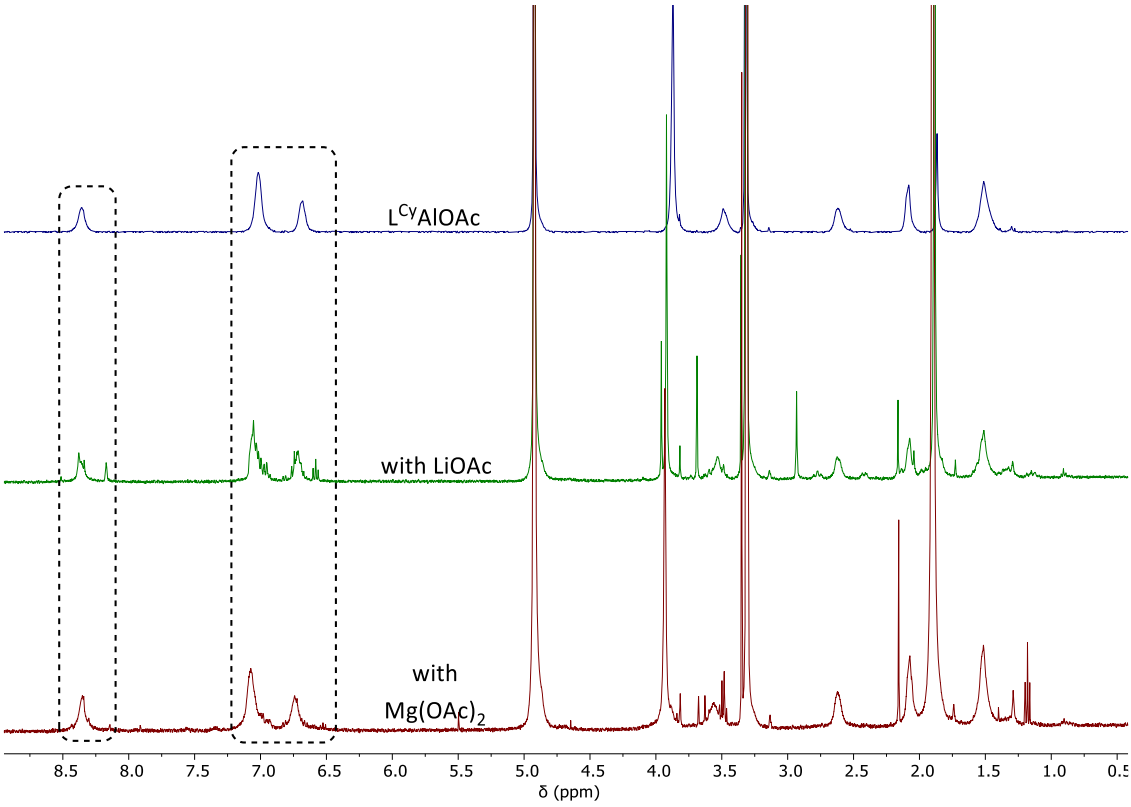

Figure S 7: Stacked ^{1}H NMR spectra (400 MHz, CD_3OD) of $L^{Cy}AlOAc$ with different metal acetates.

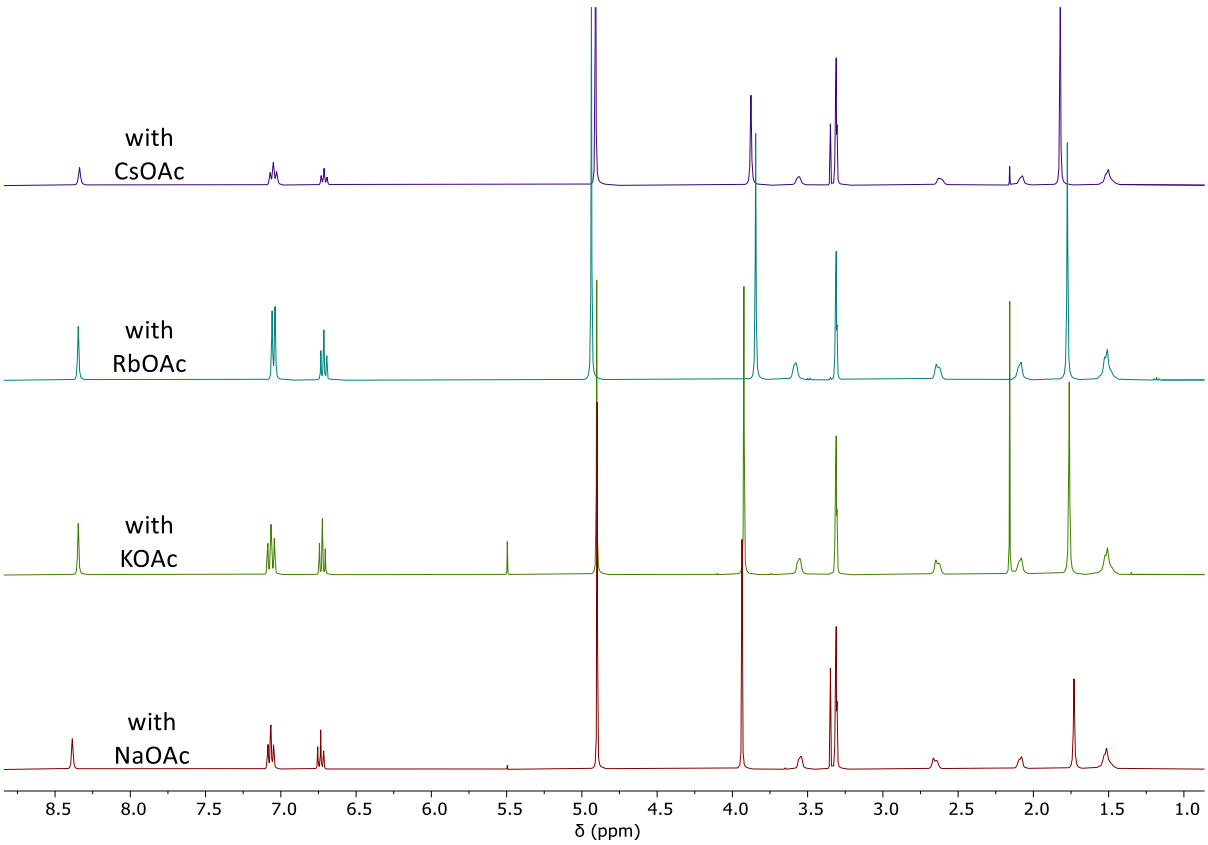

Figure S 8: Stacked ^{1}H NMR spectra (400 MHz, CD_3OD) of $L^{Cy}AlOAc$ with different metal acetates.

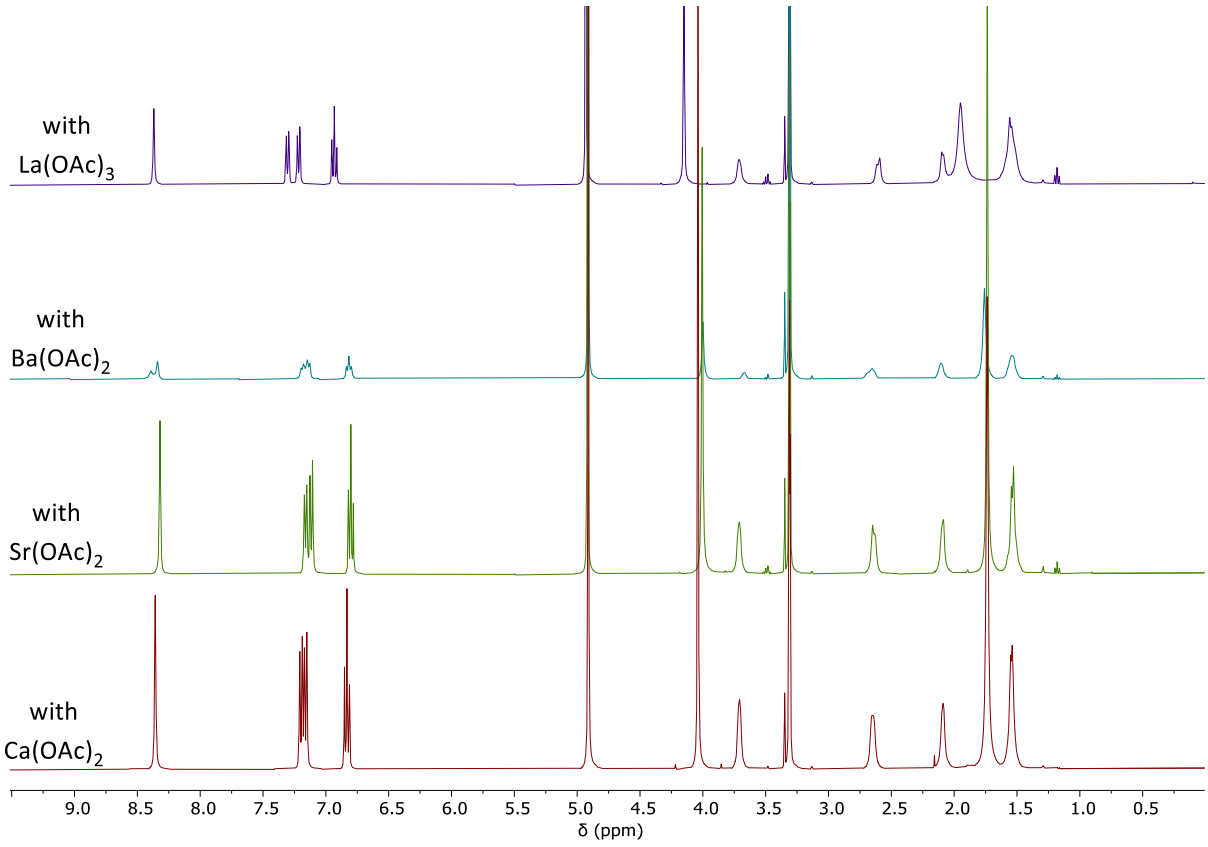

Figure S 9: Stacked ^{1}H NMR spectra (400 MHz, CD_3OD) of $L^{Cy}AlOAc$ with different metal acetates.

Section S3: ROCOP with PTA/CHO and PA/CHO

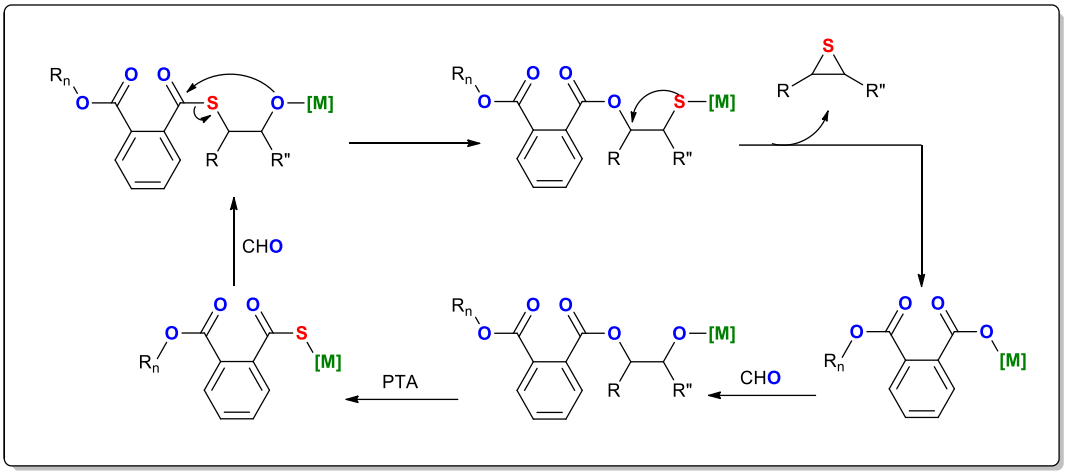

Scheme S 2: Mechanism for oxygen enrichment.

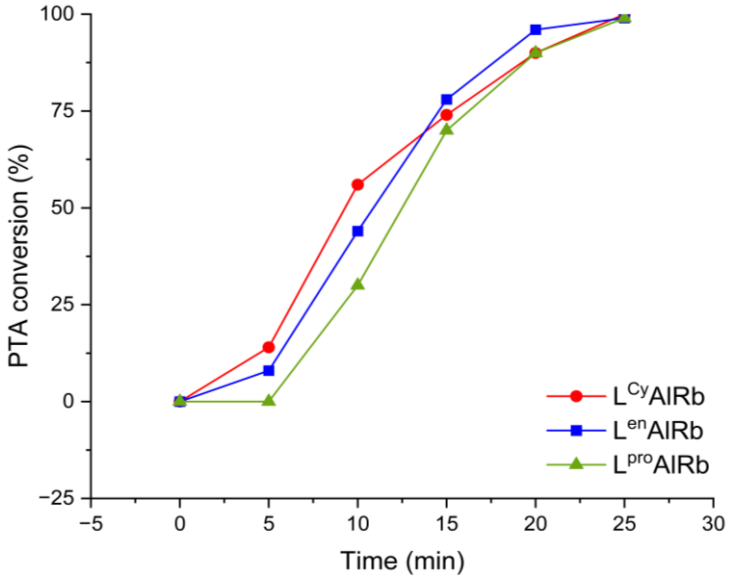

Figure S 10: PTA/CHO ROCOP showing conversion vs time plots for $L^{Cy/en/pro}Al(OAc)$ with RbOAc.

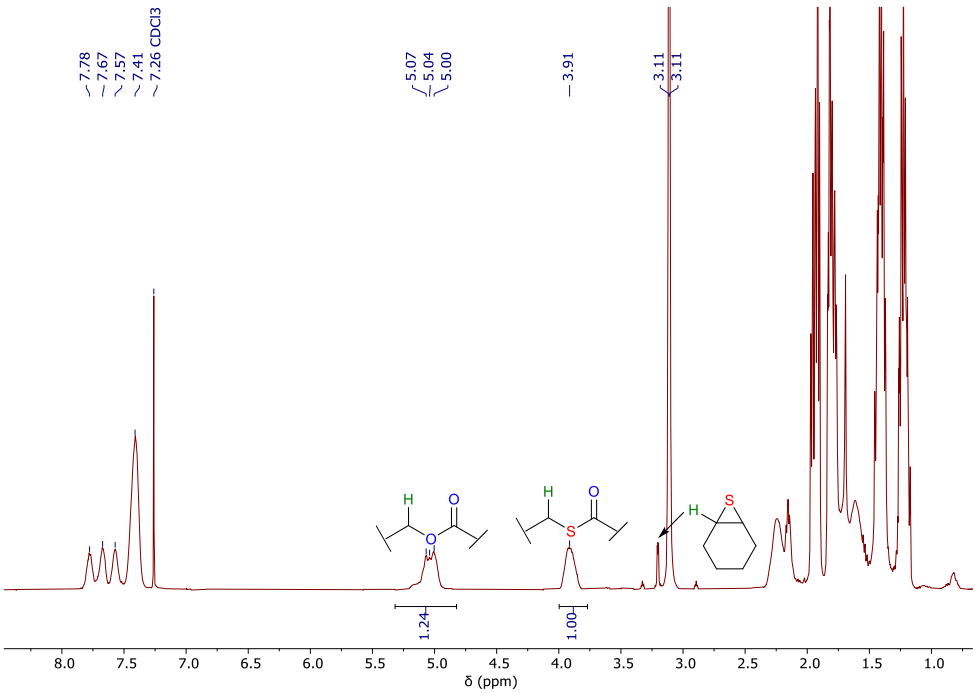

Figure S 11: ^{1}H NMR spectrum (400 MHz, $CDCl_3$) of PTA/CHO ROCOP mixture employing L^{Cy}AlOAc with RbOAc after 25 min. Near identical results were obtained with L^{Cy}AlOAc and RbOAc added separately without preforming the adduct.

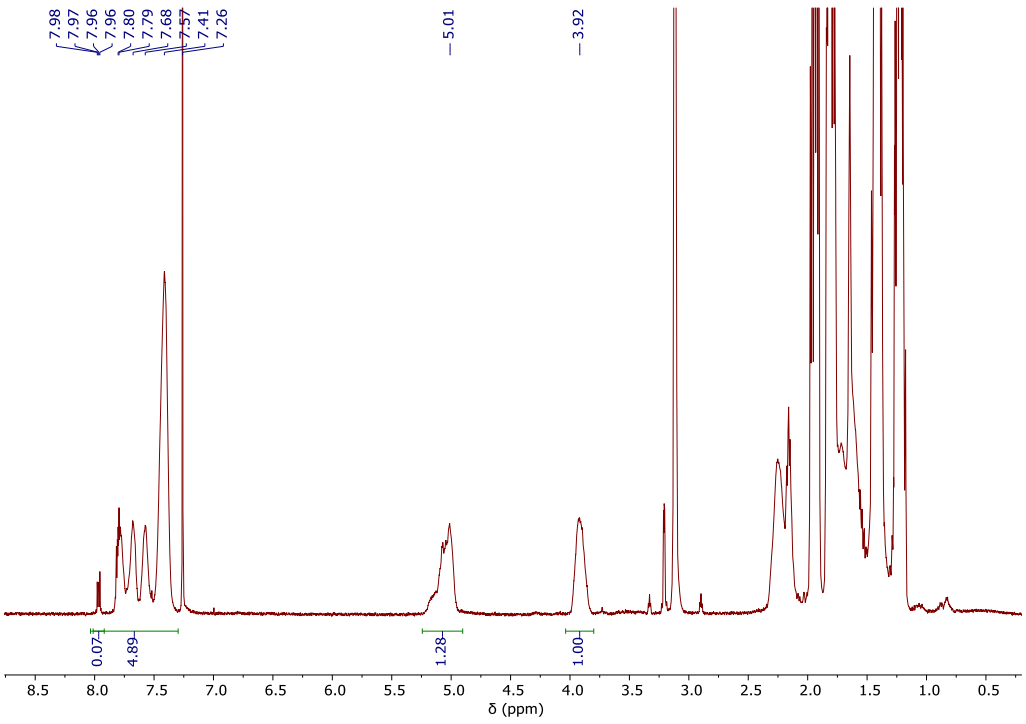

Figure S 12: ^{1}H NMR spectrum (400 MHz, $CDCl_3$) of PTA/CHO ROCOP mixture employing L^{pro}AlOAc with RbOAc after 25 min.

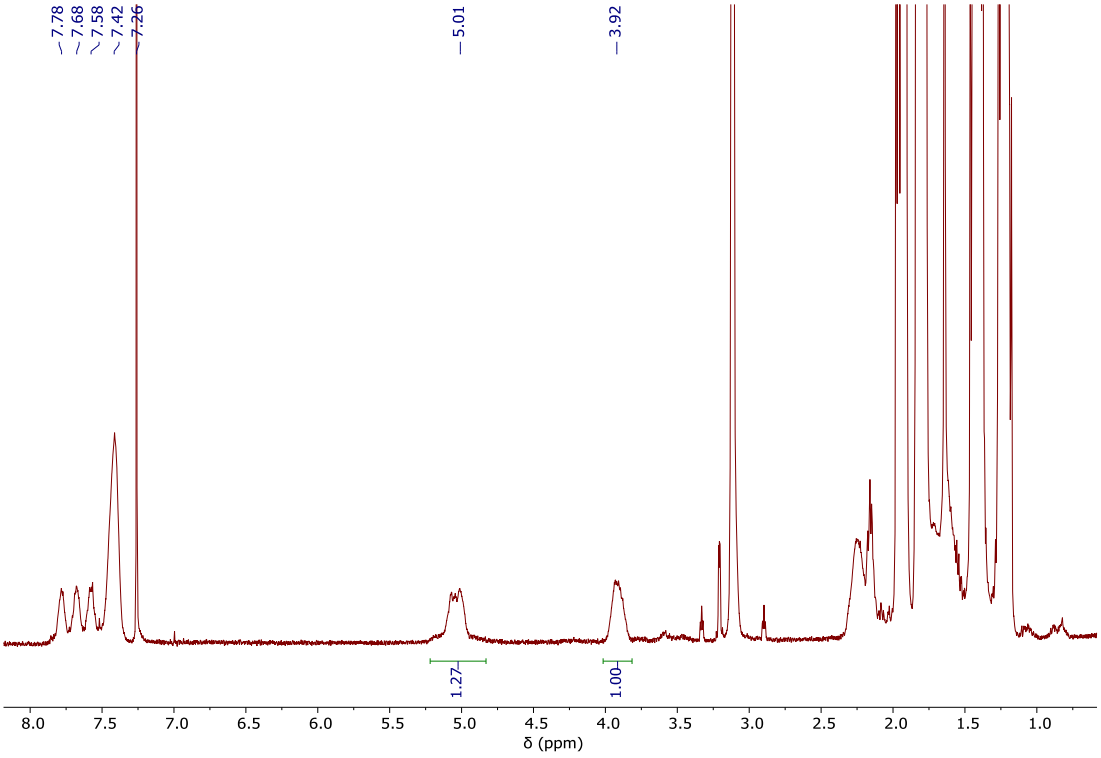

Figure S 13: ^{1}H NMR spectrum (400 MHz, $CDCl_3$) of PTA/CHO ROCOP mixture employing $L^{en}AlOAc$ with RbOAc after 25 min.

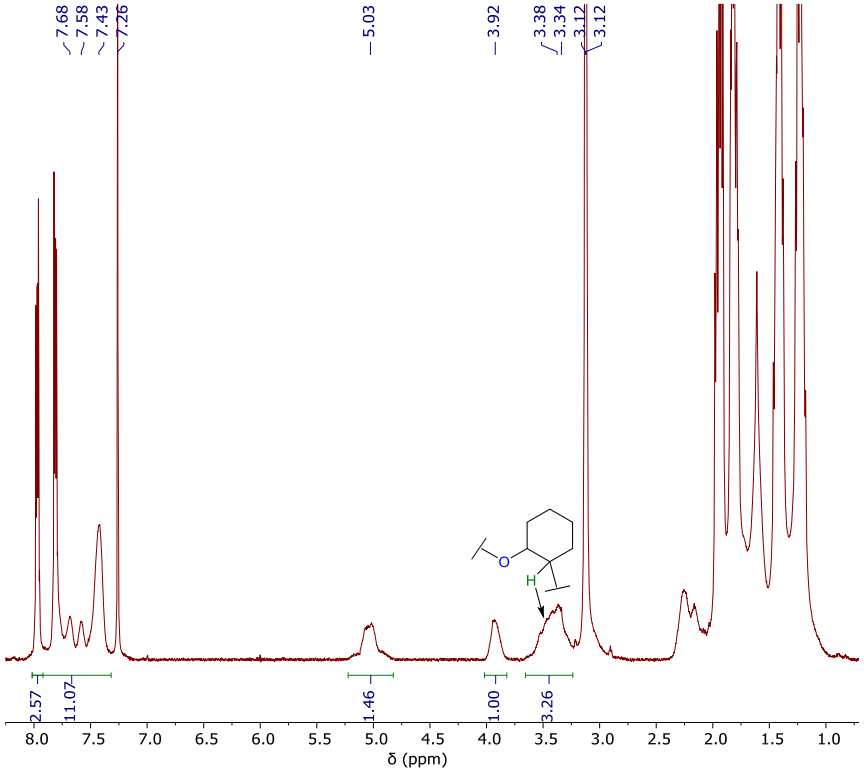

Figure S 14: ^{1}H NMR spectrum (400 MHz, $CDCl_3$) of PTA/CHO ROCOP mixture employing $L^{Ph}AlOAc$ with RbOAc after 12 h.

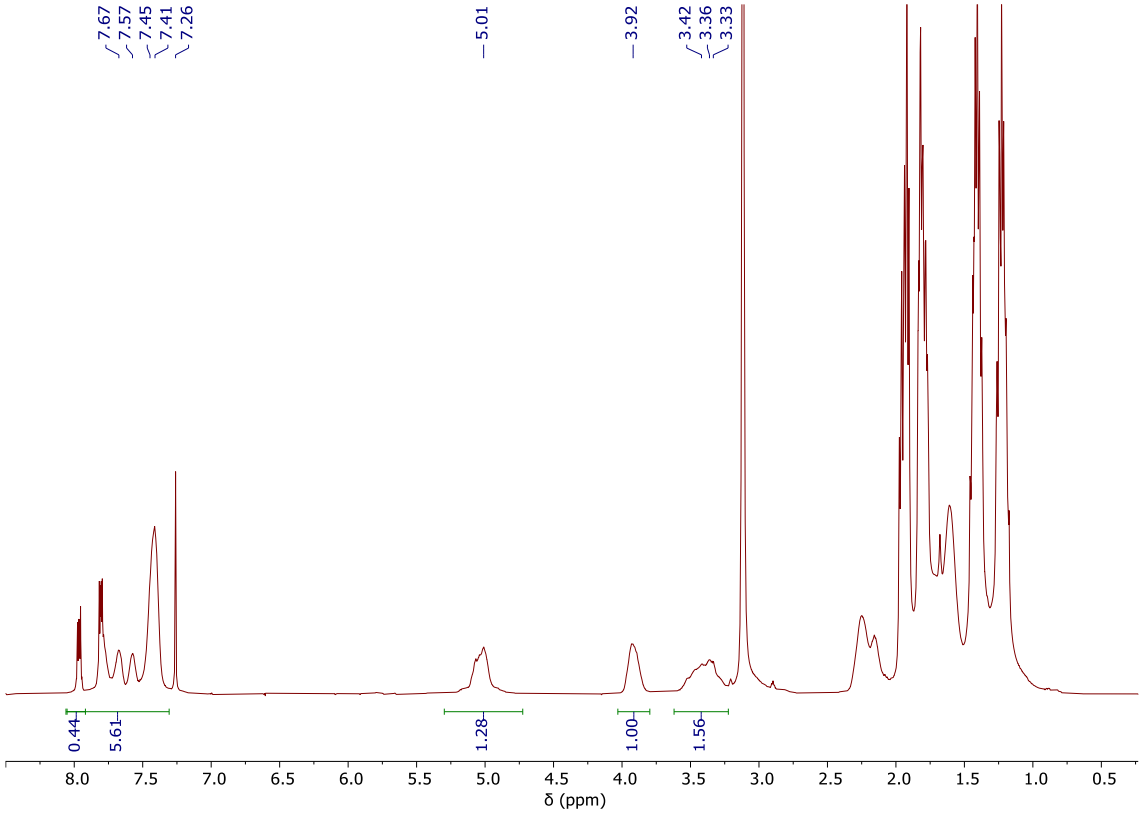

Figure S 15^{1}H NMR spectrum (400 MHz, $CDCl_3$) of PTA/CHO ROCOP mixture employing L^{Cy}AlOAc after 14 h.

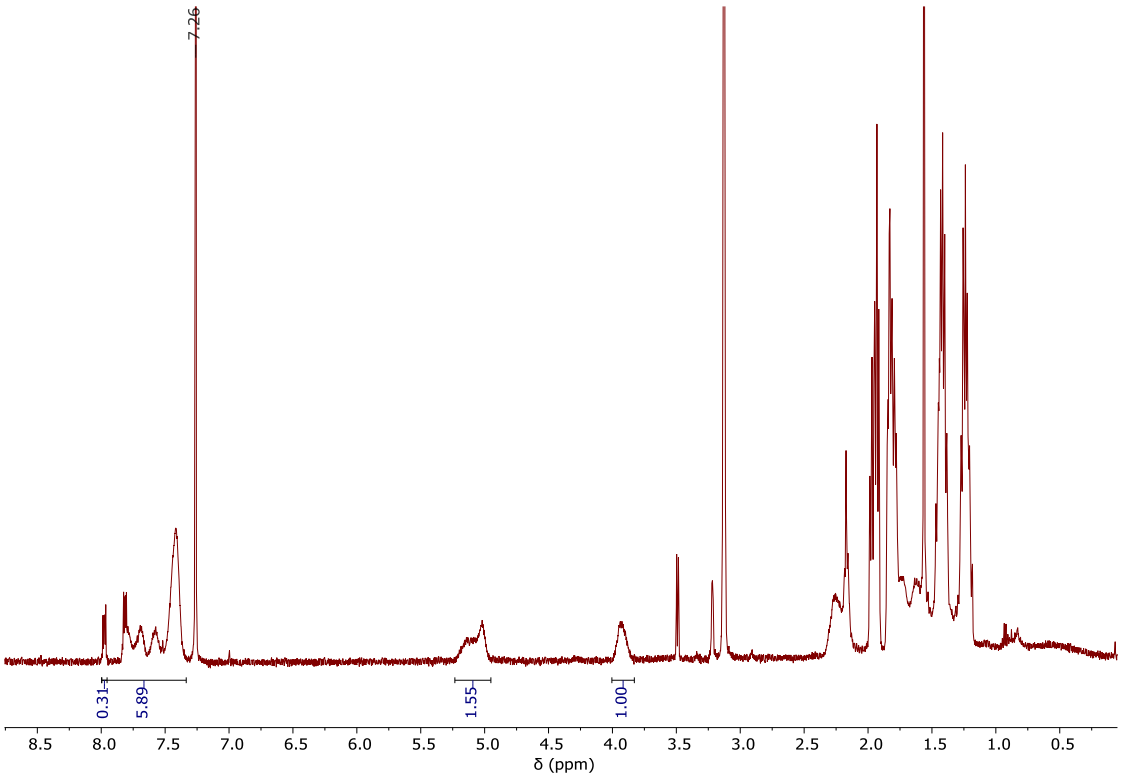

Figure S 16: ^{1}H NMR spectrum (400 MHz, $CDCl_3$) of PTA/CHO ROCOP mixture employing L^{Cy}AlOAc with LiOAc after 6 h.

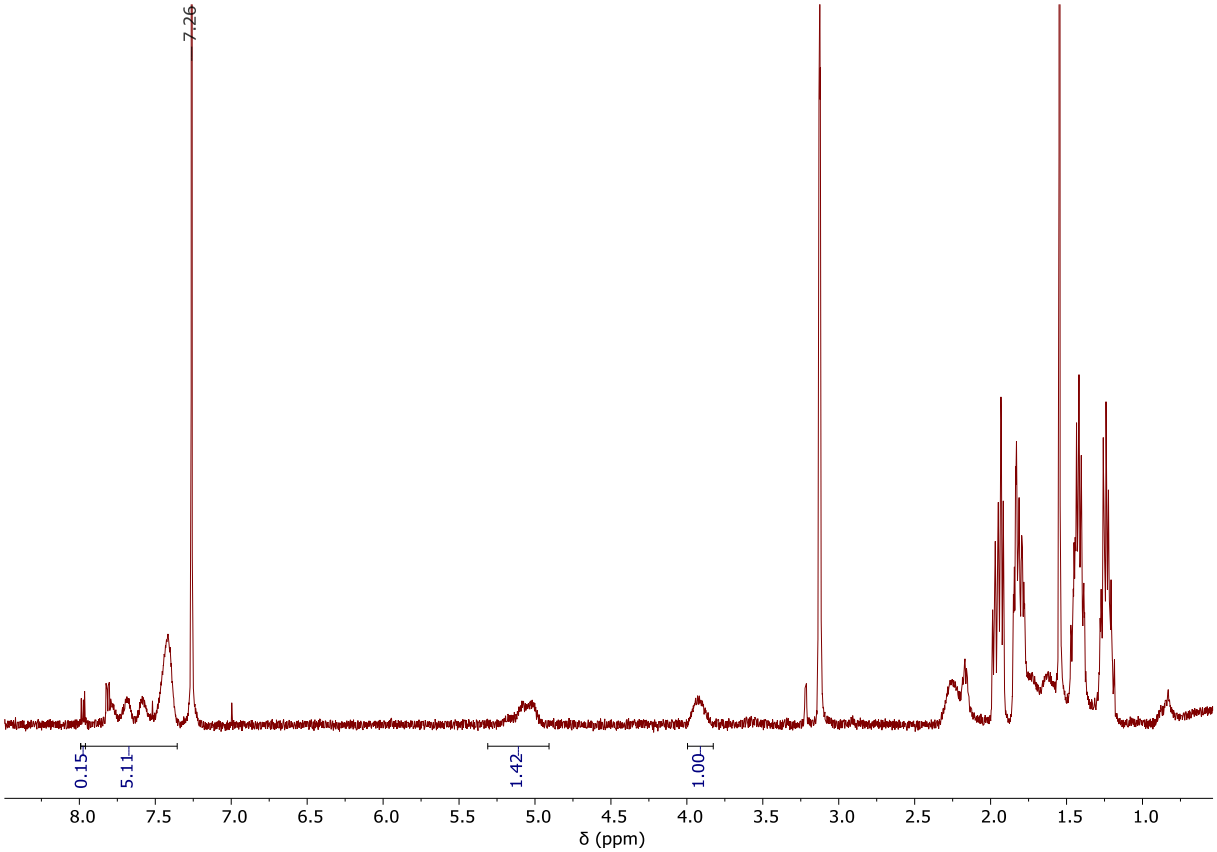

Figure S 17: ^{1}H NMR spectrum (400 MHz, $CDCl_3$) of PTA/CHO ROCOP mixture employing L^{Cy}AlOAc with NaOAc after 6 h.

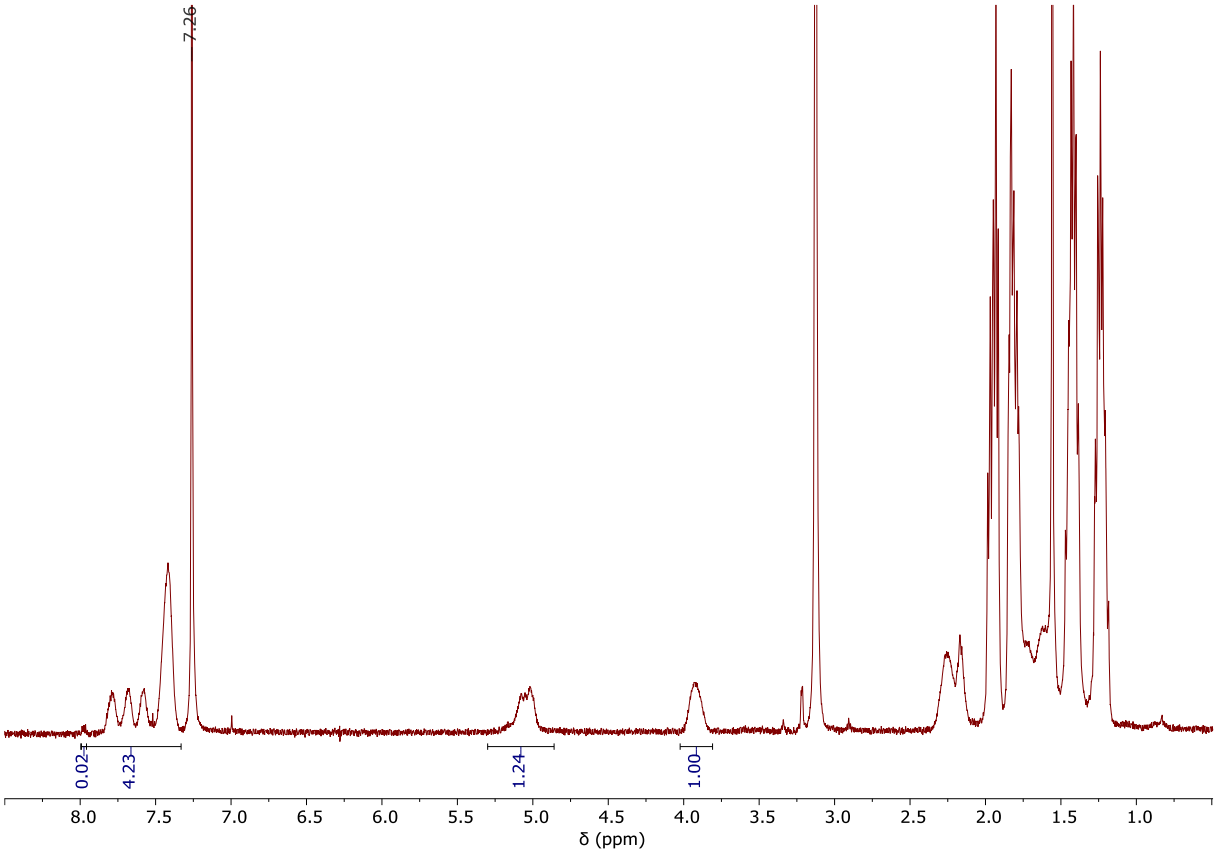

Figure S 18: ^{1}H NMR spectrum (400 MHz, $CDCl_3$) of PTA/CHO ROCOP mixture employing L^{Cy}AlOAc with KOAc after 45 min.

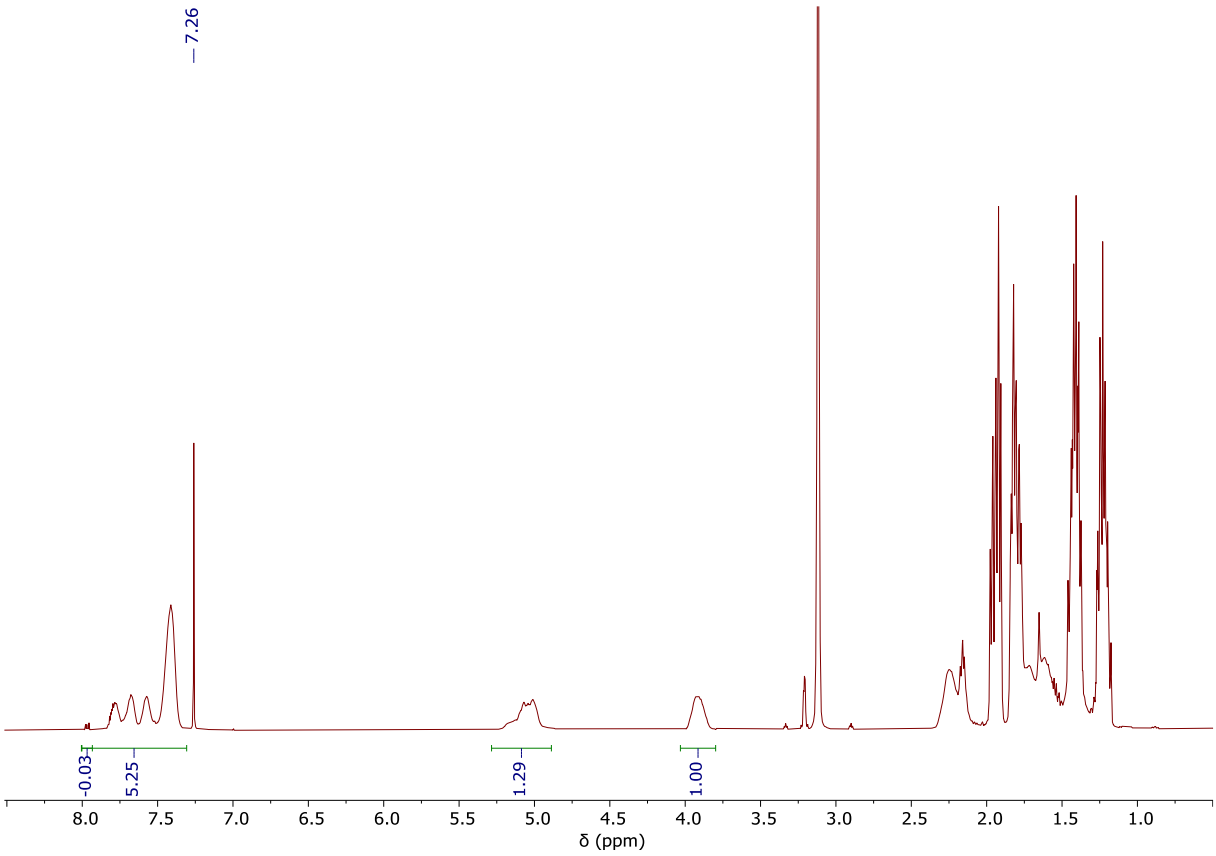

Figure S 19: ^{1}H NMR spectrum (400 MHz, $CDCl_3$) of PTA/CHO ROCOP mixture employing L^{Cy}AlOAc with CsOAc after 75 min.

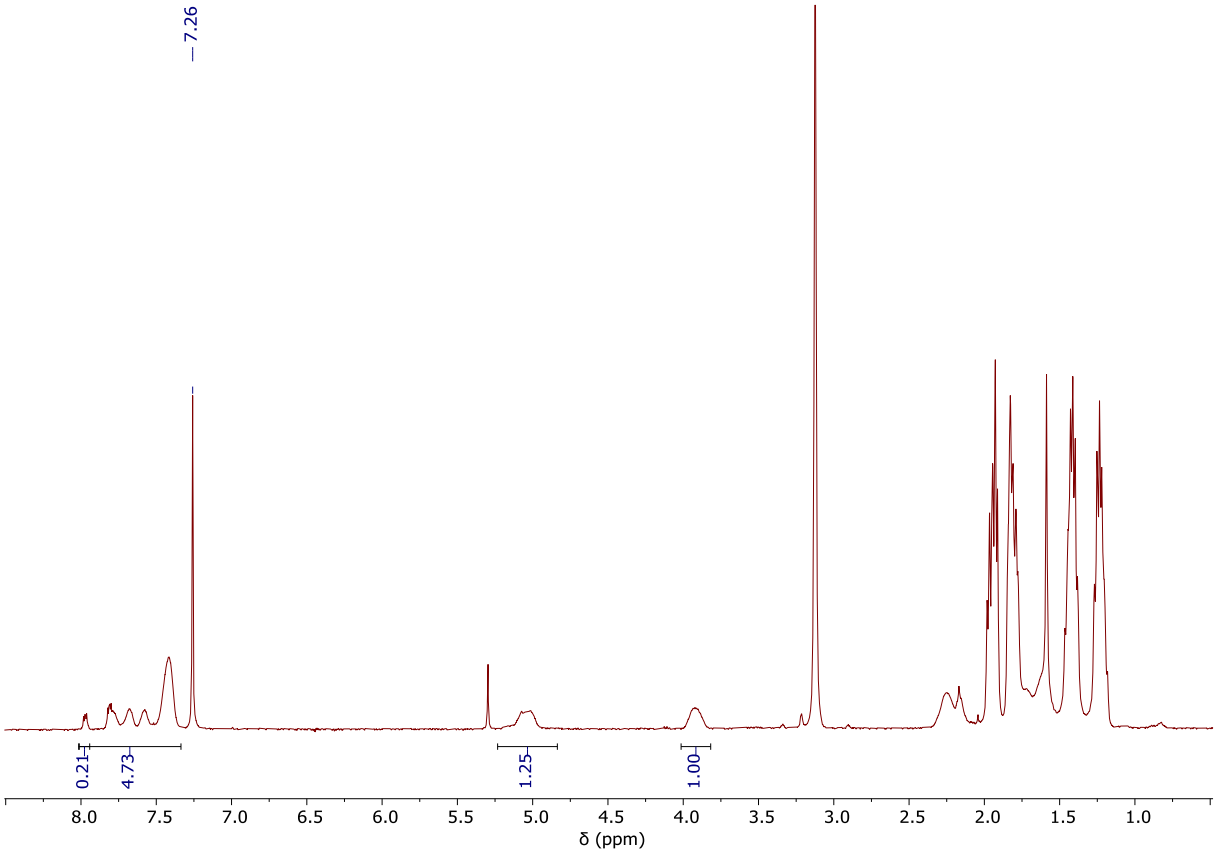

Figure S 20: ^{1}H NMR spectrum (400 MHz, $CDCl_3$) of PTA/CHO ROCOP mixture employing L^{Cy}AlOAc with $Mg(OAc)_2$ after 8 h.

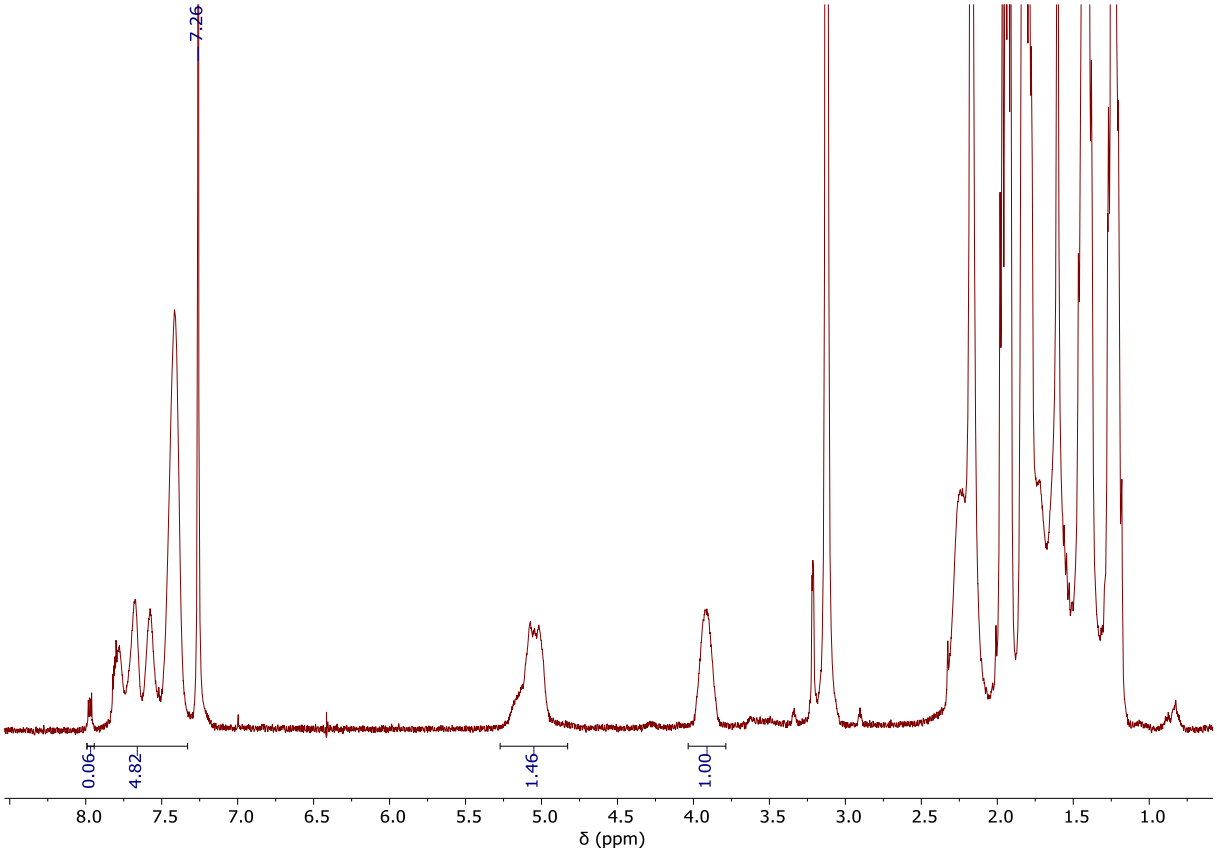

Figure S 21: ^{1}H NMR spectrum (400 MHz, $CDCl_3$) of PTA/CHO ROCOP mixture employing $L^{Cy}AlOAc$ with $Ca(OAc)_2$ after 5.5 h.

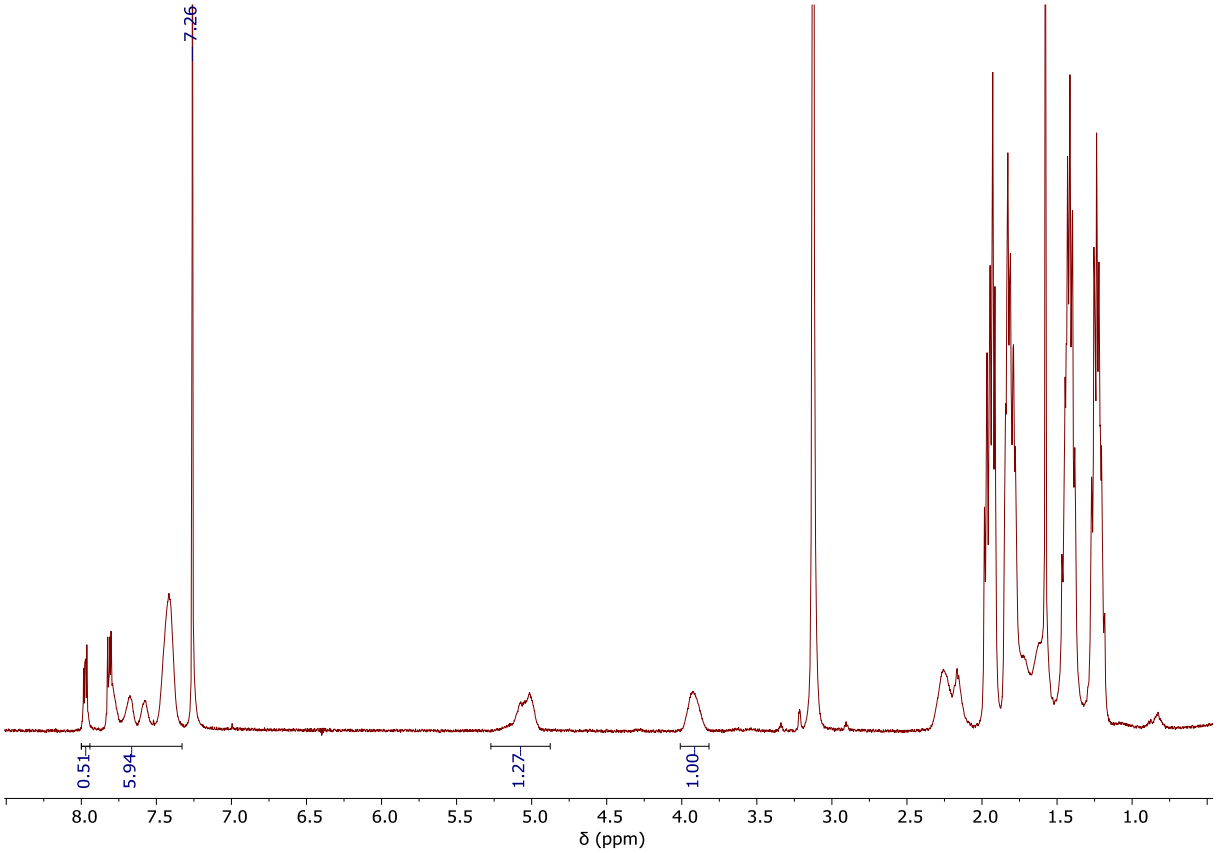

Figure S 22: ^{1}H NMR spectrum (400 MHz, $CDCl_3$) of PTA/CHO ROCOP mixture employing $L^{Cy}AlOAc$ with $Sr(OAc)_2$ after 5.5 h.

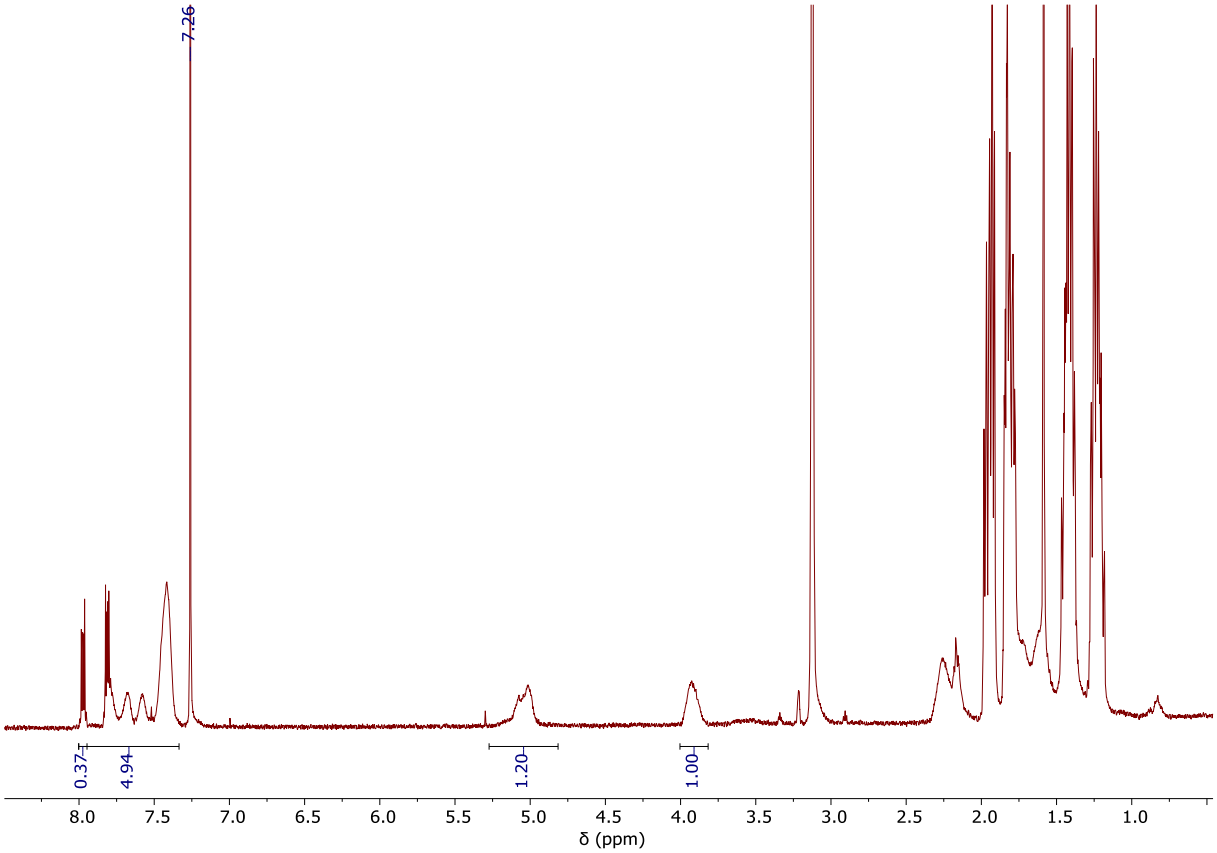

Figure S 23: ^{1}H NMR spectrum (400 MHz, $CDCl_3$) of PTA/CHO ROCOP mixture employing $L^{Cy}AlOAc$ with $Ba(OAc)_2$ after 10 h.

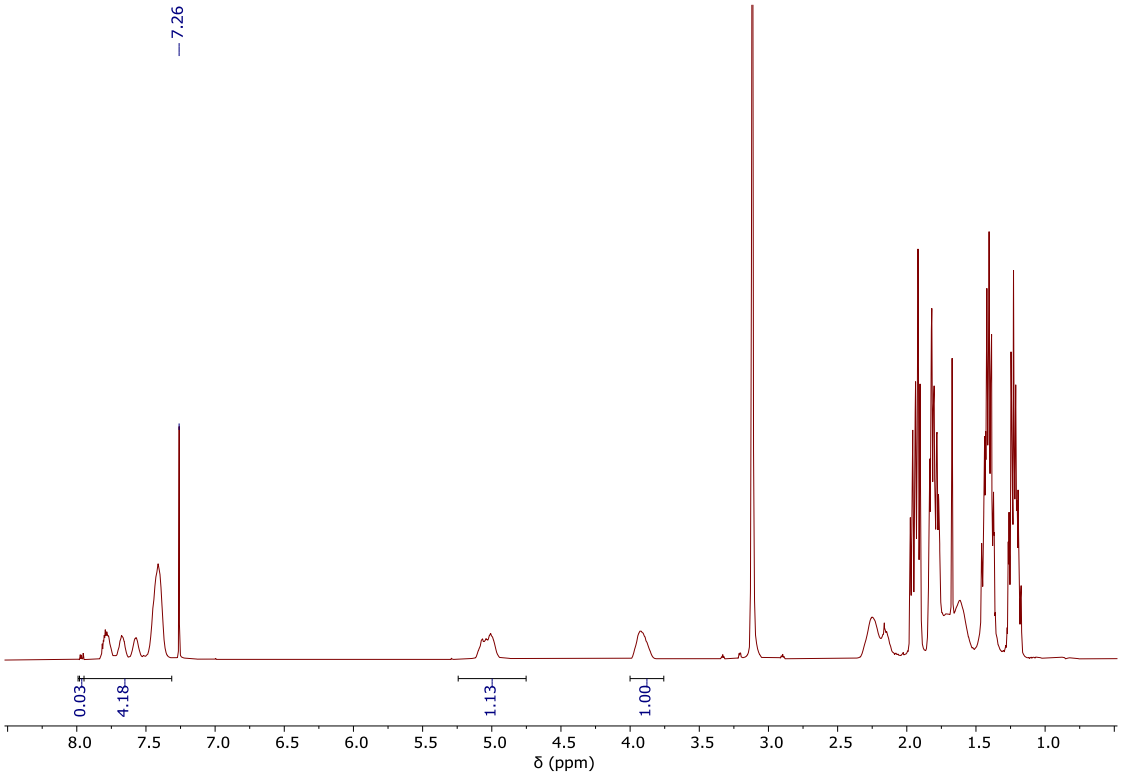

Figure S 24: ^{1}H NMR spectrum (400 MHz, $CDCl_3$) of PTA/CHO ROCOP mixture employing $L^{Cy}AlOAc$ with $La(OAc)_3$ after 2.5 h.

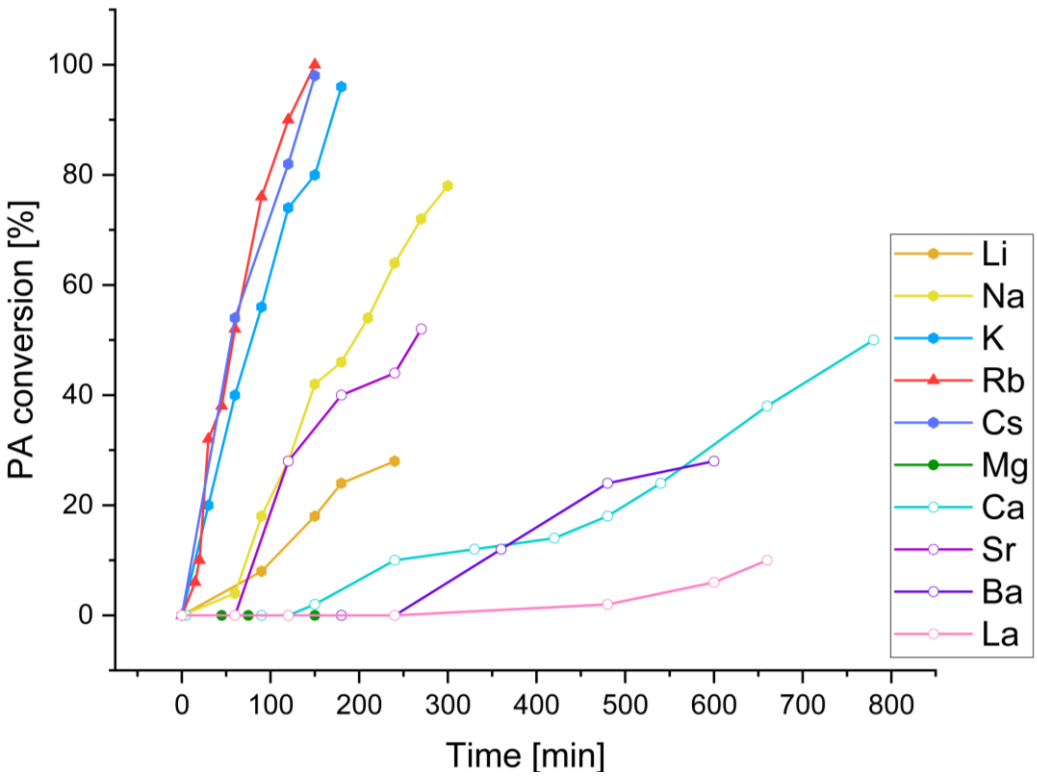

Figure S 25: PA/CHO ROCOP conversion vs time plots corresponding to Table 1.

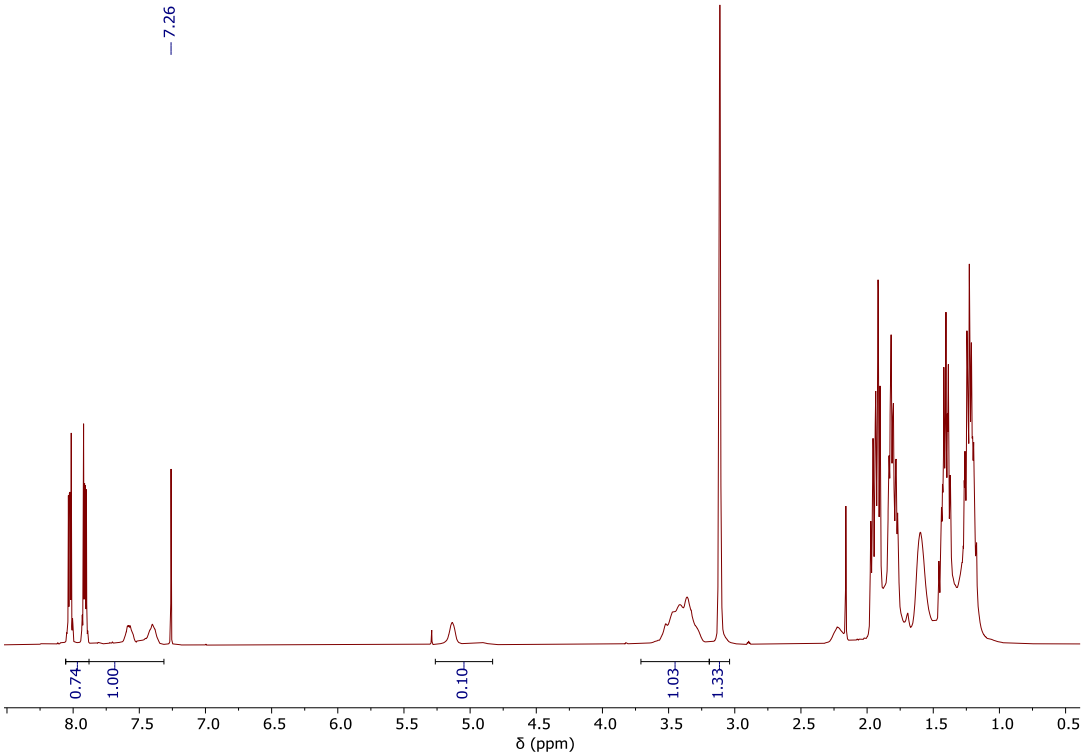

Figure S 26: ^{1}H NMR spectrum (400 MHz, $CDCl_3$) of PA/CHO ROCOP mixture employing $L^{Cy}AlOAc$ with LiOAc after 4 h.

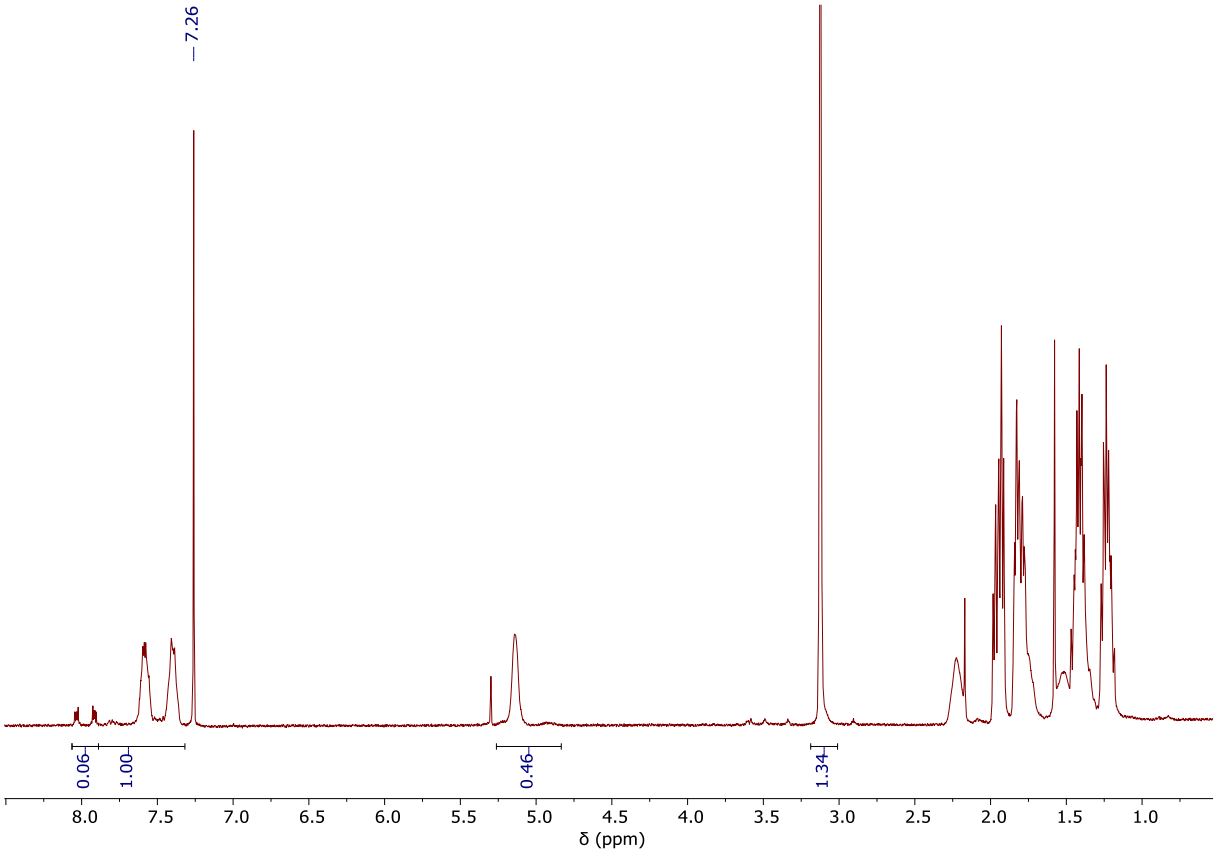

Figure S 27: ^{1}H NMR spectrum (400 MHz, $CDCl_3$) of PA/CHO ROCOP mixture employing L^{Cy}AlOAc with NaOAc after 10 h.

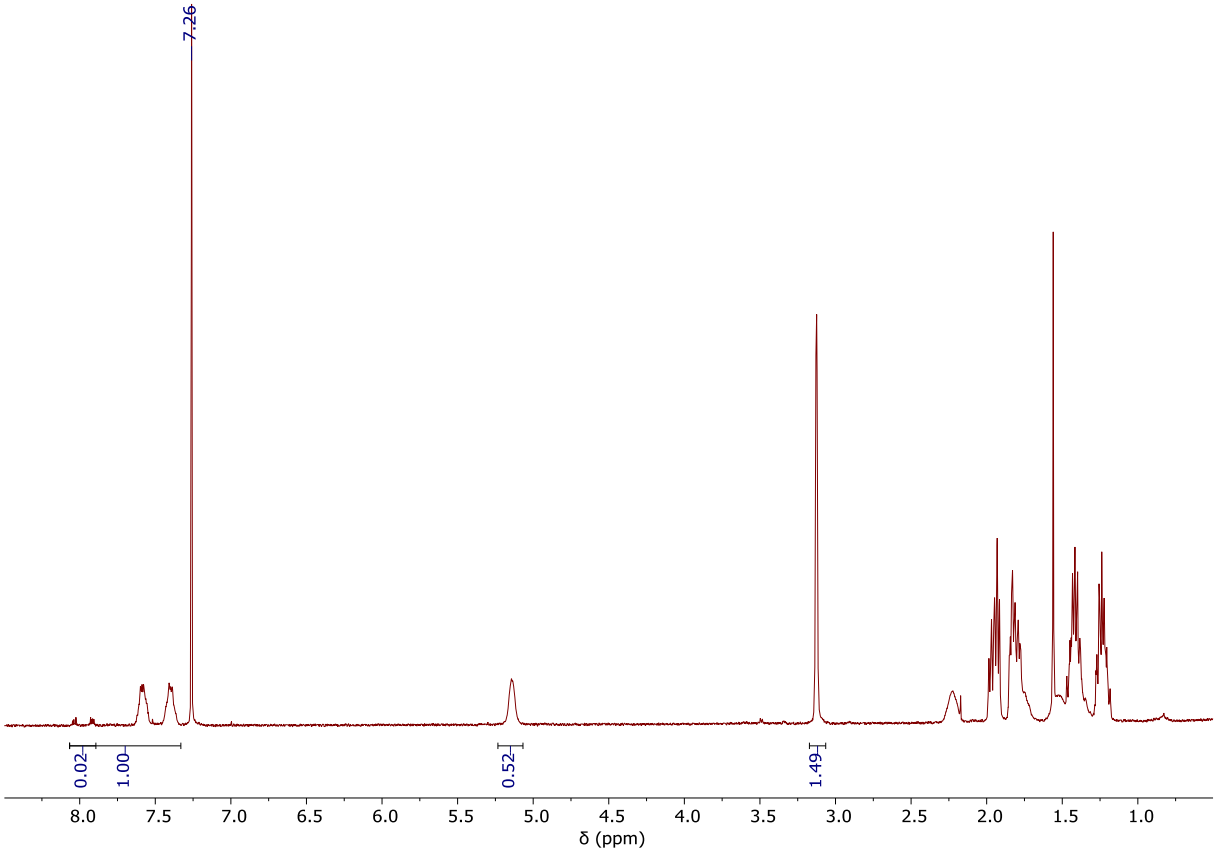

Figure S 28: ^{1}H NMR spectrum (400 MHz, $CDCl_3$) of PA/CHO ROCOP mixture employing L^{Cy}AlOAc with KOAc after 3 h.

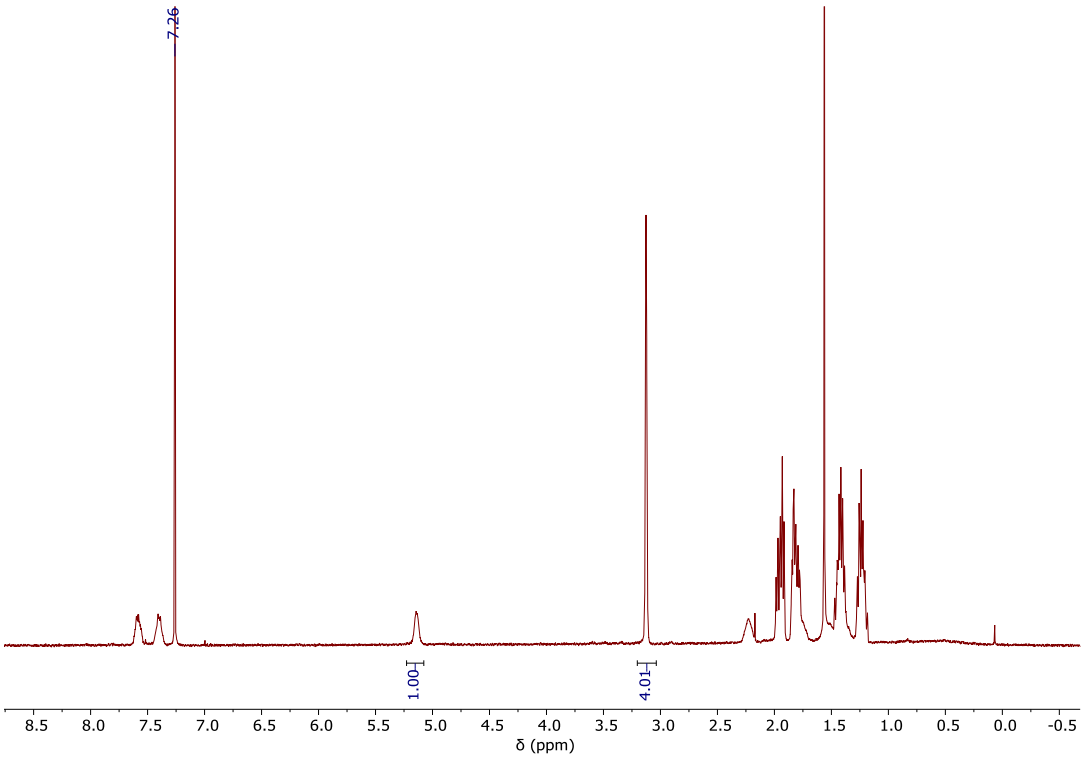

Figure S 29: ^{1}H NMR spectrum (400 MHz, $CDCl_3$) of PA/CHO ROCOP mixture employing L^{Cy}AlOAc with RbOAc after 2.5 h.

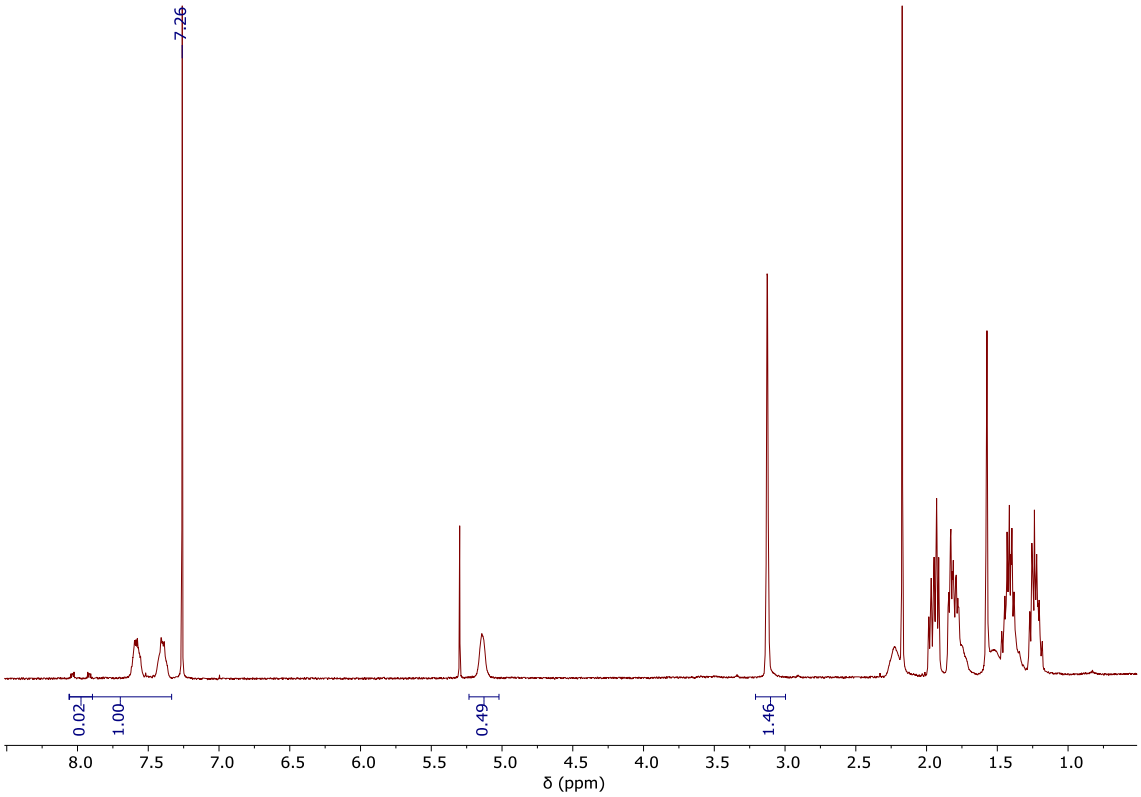

Figure S 30: ^{1}H NMR spectrum (400 MHz, $CDCl_3$) of PA/CHO ROCOP mixture employing L^{Cy}AlOAc with CsOAc after 2.5 h.

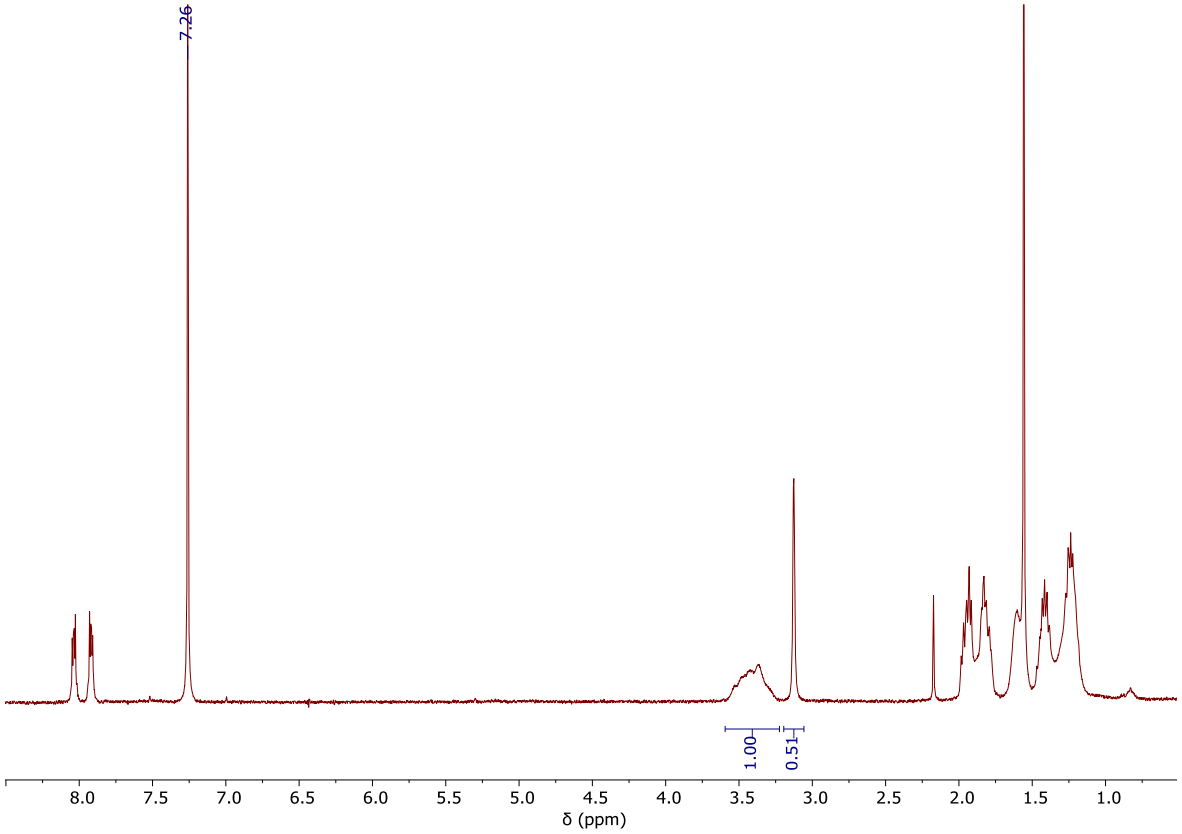

Figure S 31: ^{1}H NMR spectrum (400 MHz, $CDCl_3$) of PA/CHO ROCOP mixture employing $L^{Cy}AlOAc$ with $Mg(OAc)_2$ after 2 h.

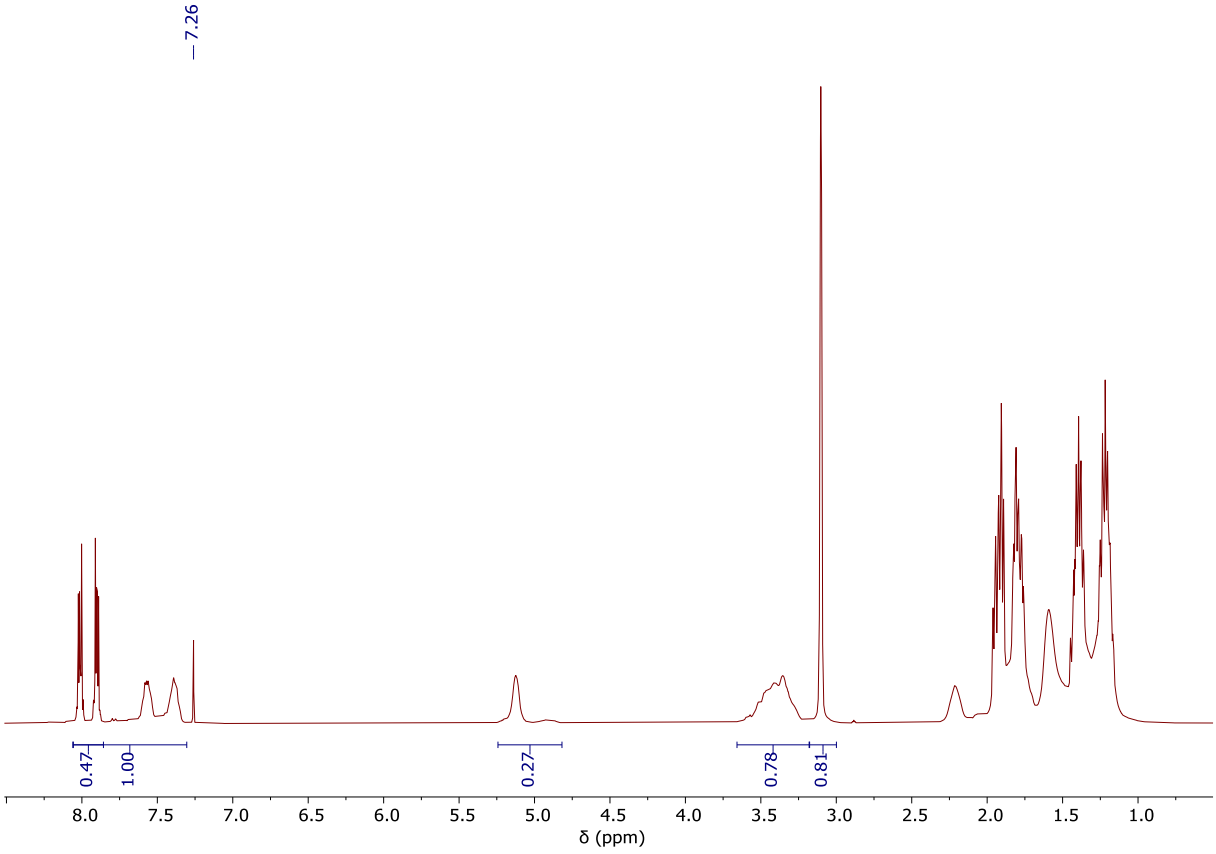

Figure S 32: ^{1}H NMR spectrum (400 MHz, $CDCl_3$) of PA/CHO ROCOP mixture employing $L^{Cy}AlOAc$ with $Ca(OAc)_2$ after 13 h.

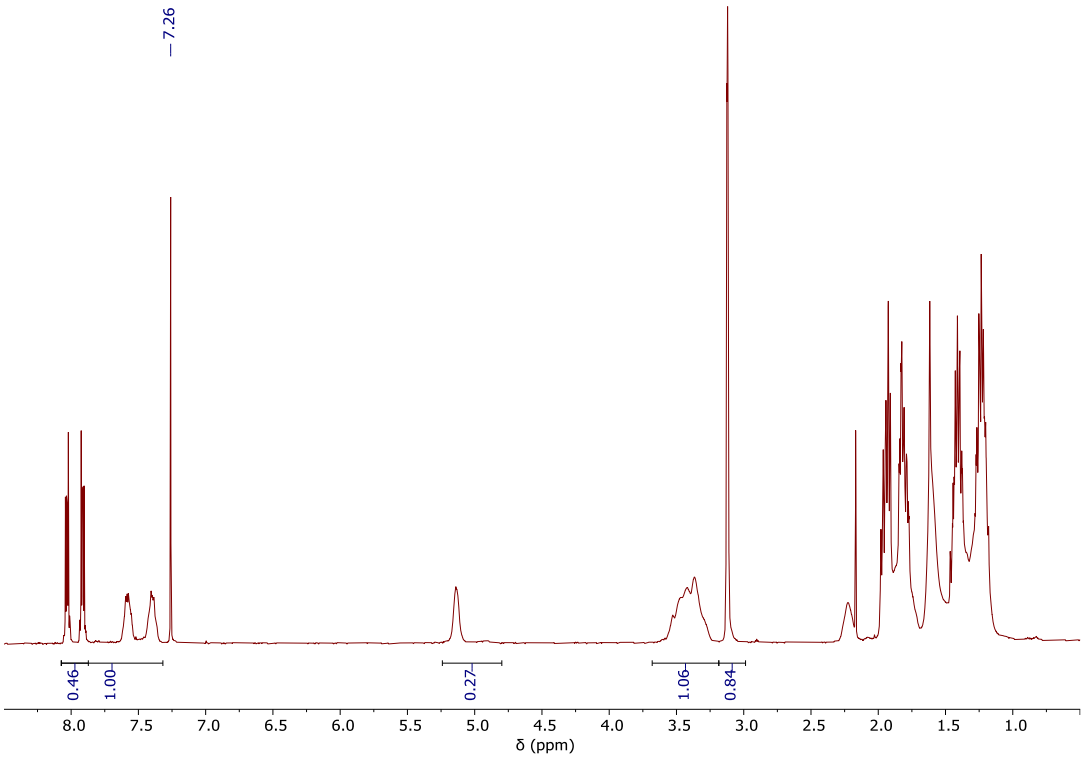

Figure S 33: ^{1}H NMR spectrum (400 MHz, $CDCl_3$) of PA/CHO ROCOP mixture employing $L^{Cy}AlOAc$ with $Sr(OAc)_2$ after 4.5 h.

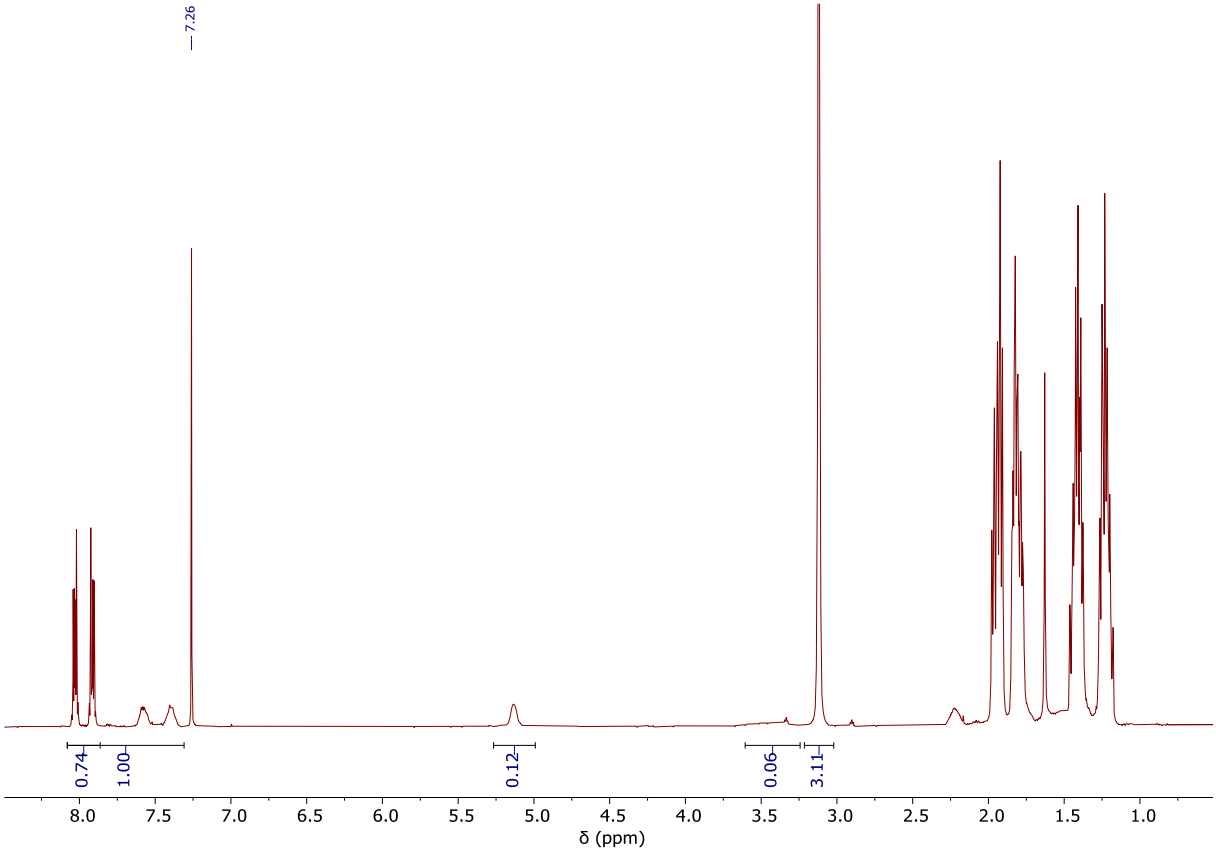

Figure S 34: ^{1}H NMR spectrum (400 MHz, $CDCl_3$) of PA/CHO ROCOP mixture employing $L^{Cy}AlOAc$ with $Ba(OAc)_2$ after 10 h.

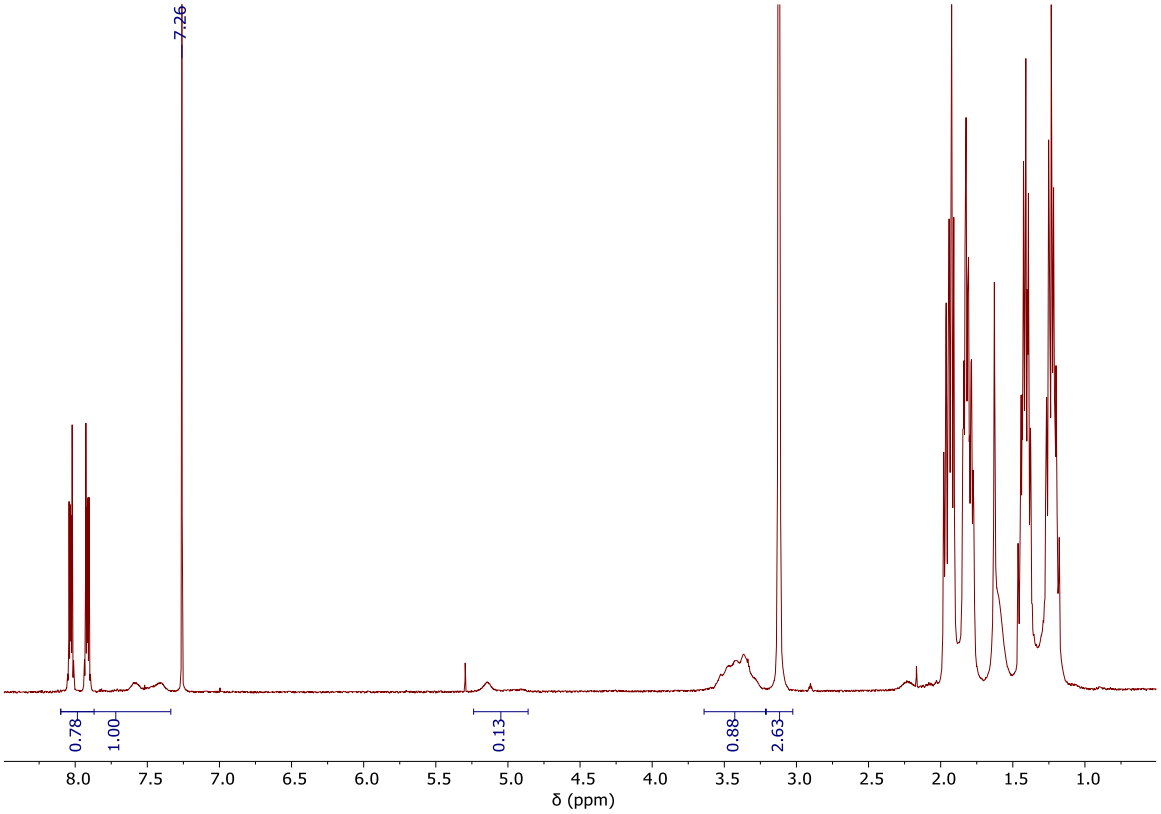

Figure S 35: ^{1}H NMR spectrum (400 MHz, $CDCl_3$) of PA/CHO ROCOP mixture employing $L^{Cy}AlOAc$ with $La(OAc)_2$ after 10 h.

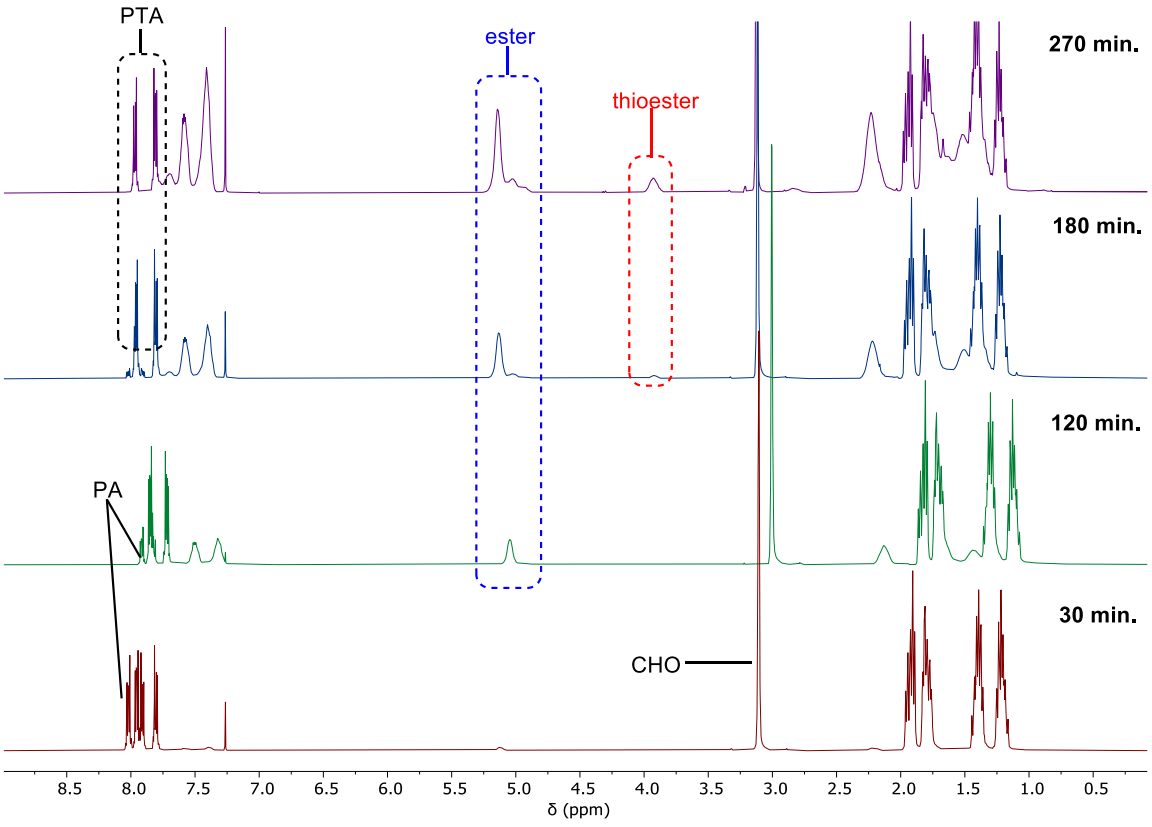

Figure S 36: Stacked ^{1}H NMR spectra (400 MHz, $CDCl_3$) of aliquots from PA/PTA/CHO ROTERP showing PA consumption before PTA.

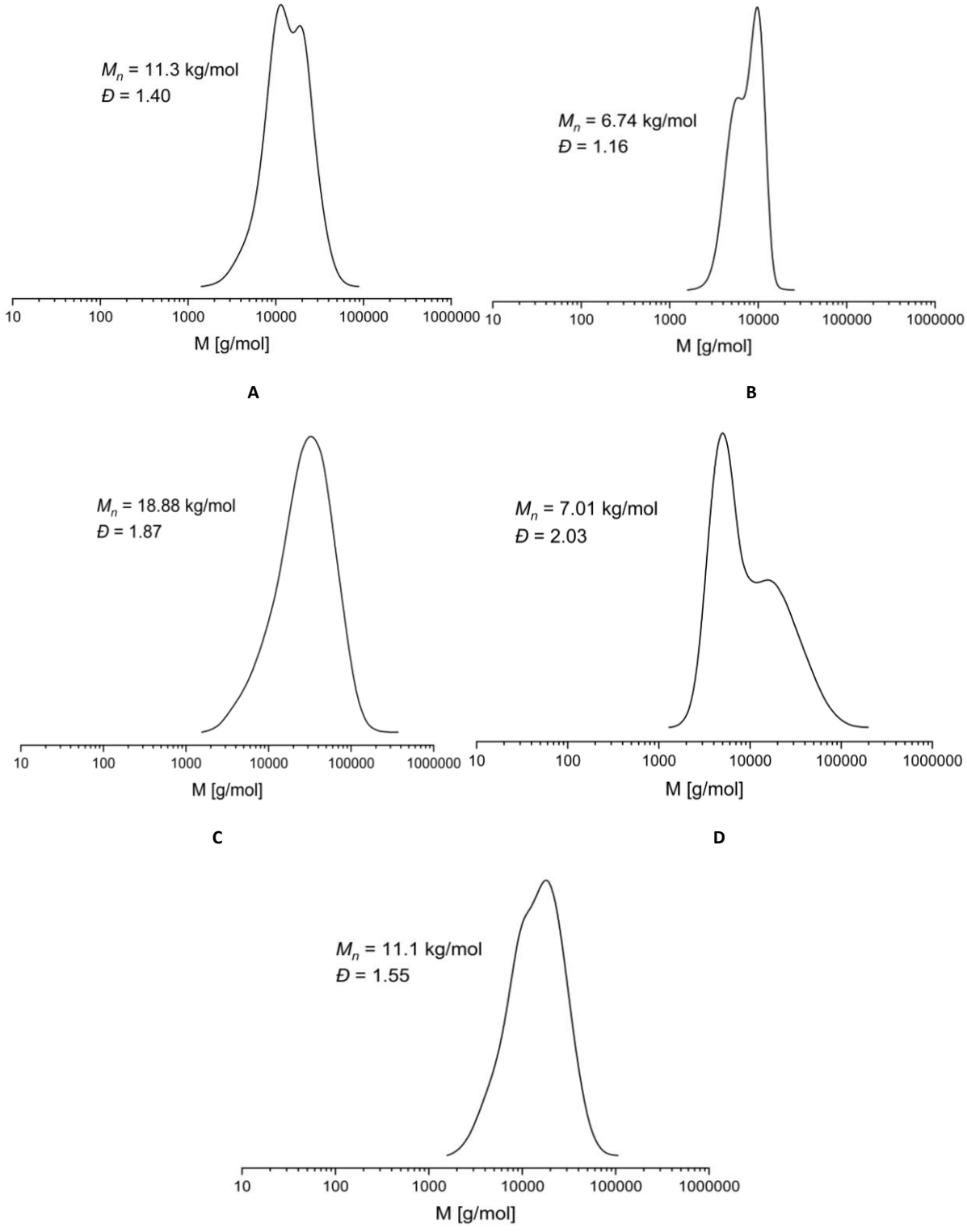

Figure S 37: GPC traces of **A**) PTA/CHO ROCOP employing L^{Cy}AlOAc with RbOAc ; **B**) PA/CHO ROCOP employing L^{Cy}AlOAc with RbOAc; **C**) PA/CHO ROCOP employing L^{Cy}AlOAc with $Mg(OAc)_2$; **D**) PA/CHO ROCOP employing L^{Cy}AlOAc with $Ca(OAc)_2$; **E)** PA/PTA/CHO ROTERP.

Section S4: ROCOP with PTA/vCHO

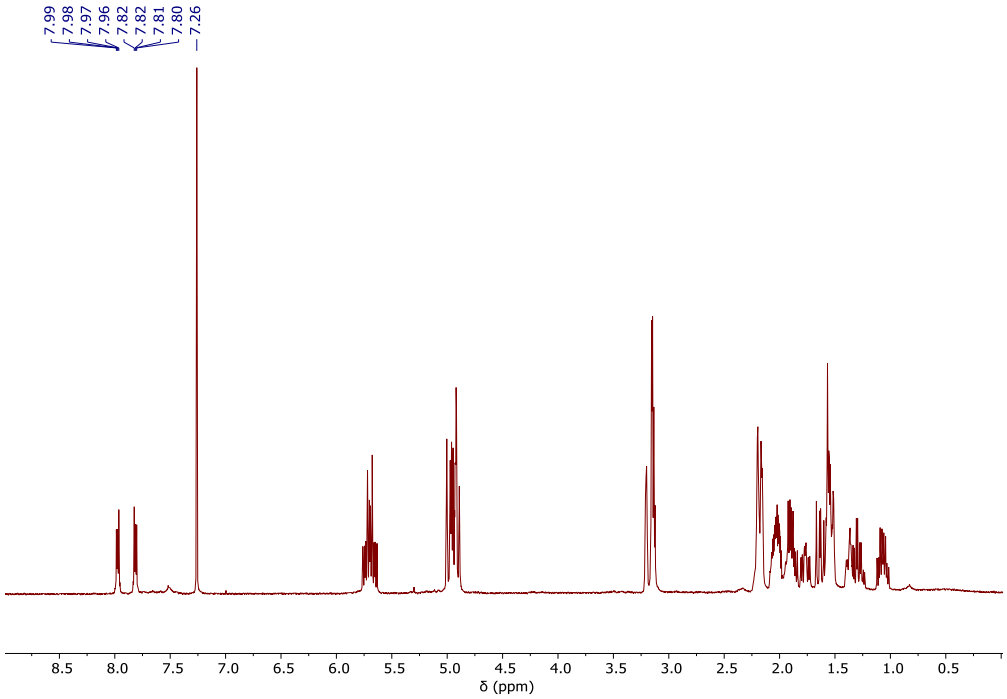

Figure S 38: ^{1}H NMR spectrum (400 MHz, $CDCl_3$) of PTA/vCHO ROCOP mixture employing L^{Cy}CrOAc with RbOAc after 24 h at 80 °C showing negligible signals from polymer formation.

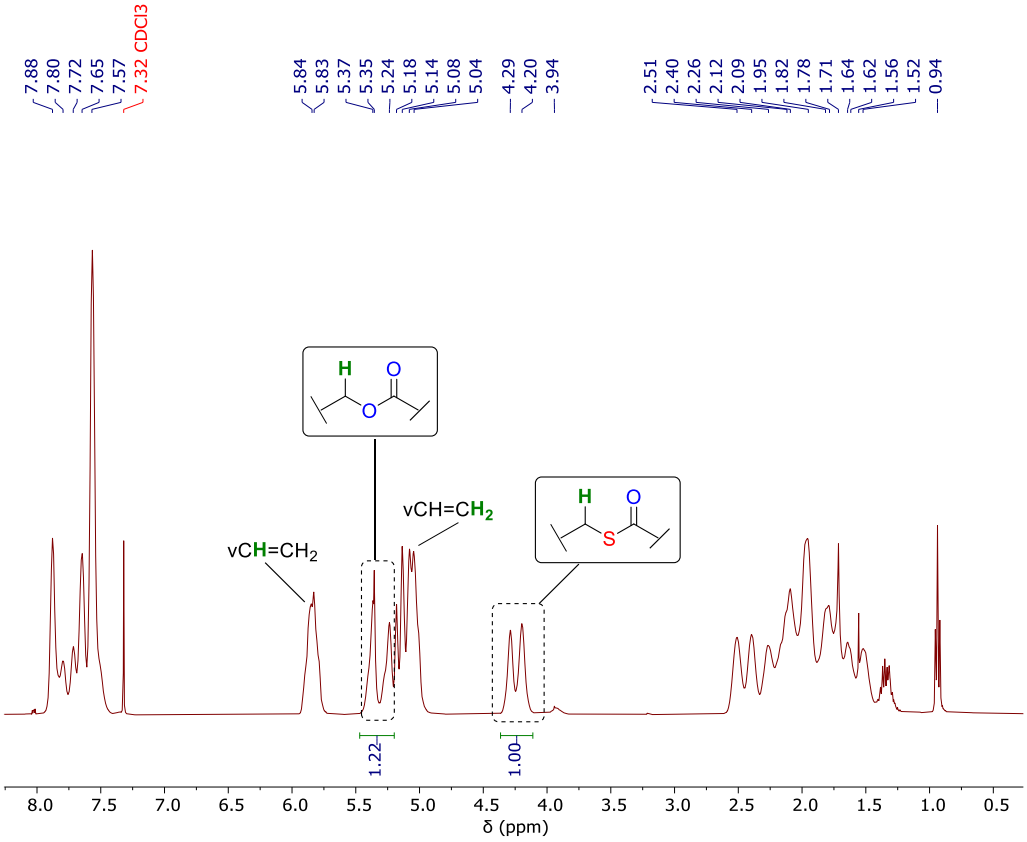

Figure S 39: ^{1}H NMR spectrum (400 MHz, $CDCl_3$) of isolated PTA/vCHO copolymer employing L^{Cy}AlOAc with RbOAc. Residual pentane from purification at 1.3 and 0.9 ppm.

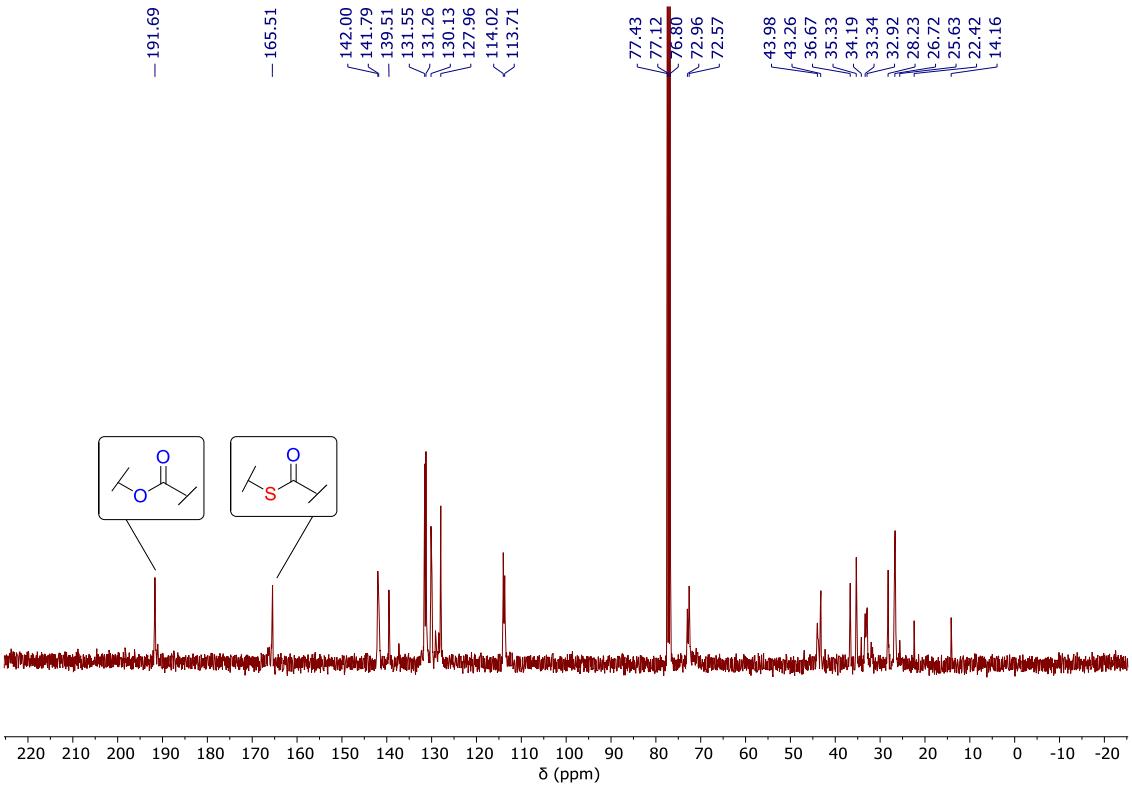

Figure S 40: ^{13}C NMR spectrum (126 MHz, $CDCl_3$) of isolated PTA/vCHO copolymer.

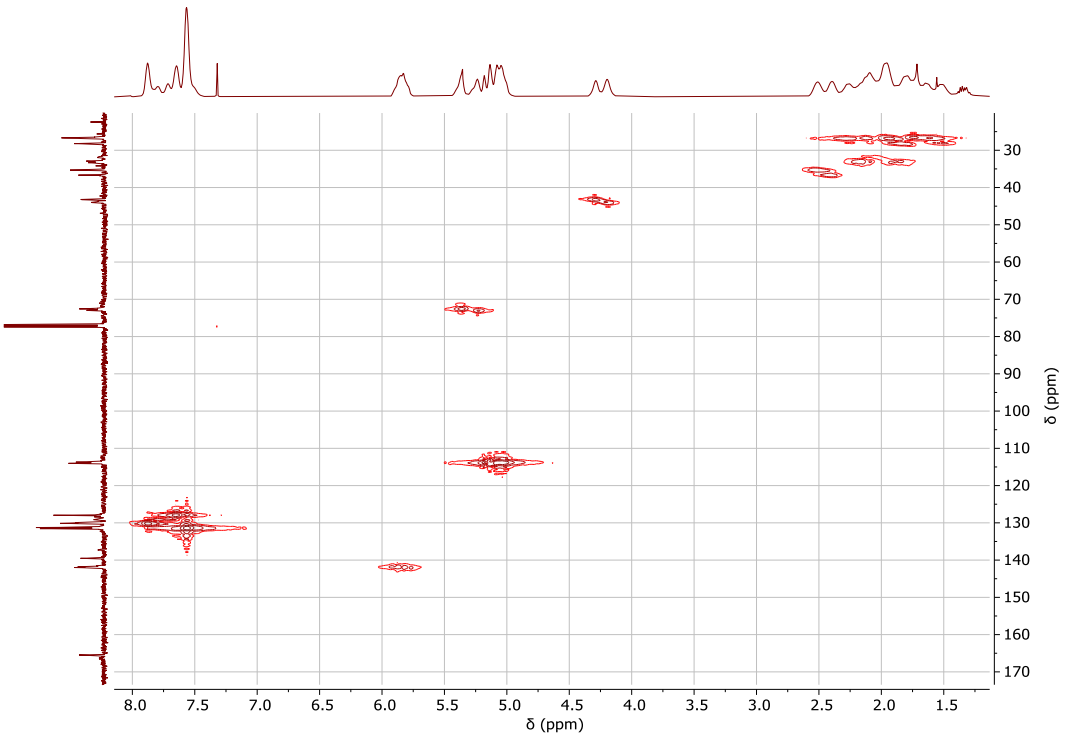

Figure S 41: ^{1}H - ^{13}C HMQC NMR spectrum ($CDCl_3$) of isolated PTA/vCHO copolymer.

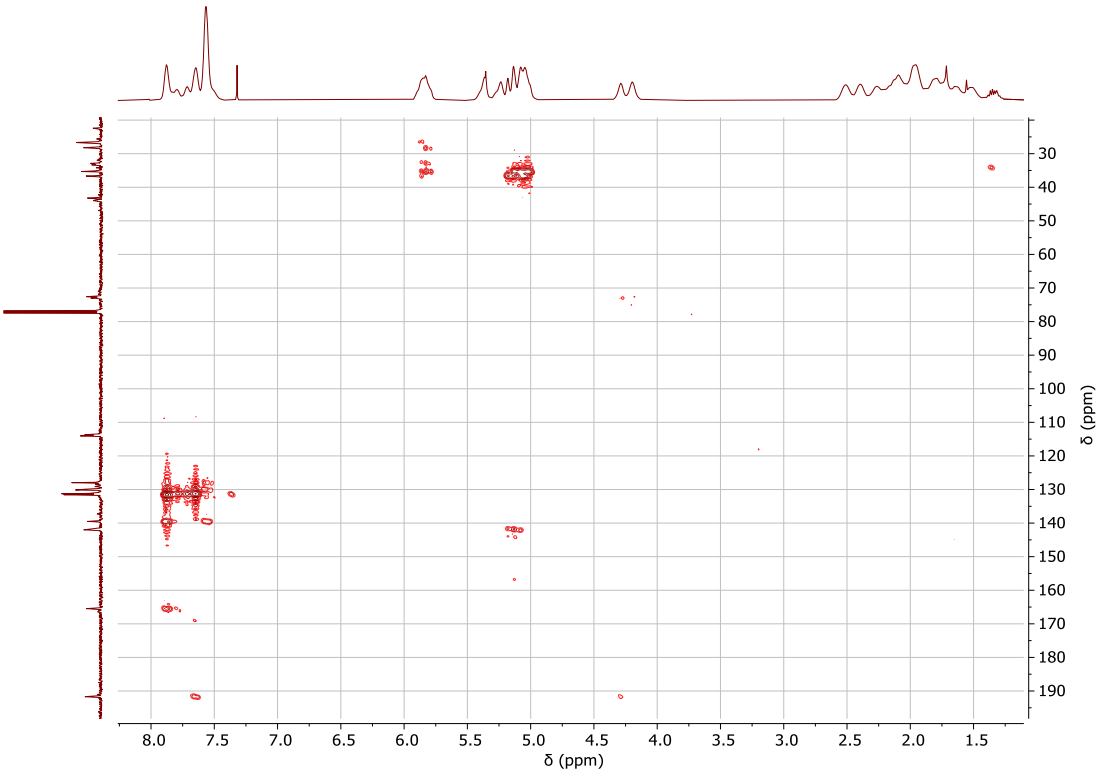

Figure S 42: ^{1}H - ^{13}C HMBC NMR spectrum ($CDCl_3$) of PTA-vCHO copolymer.

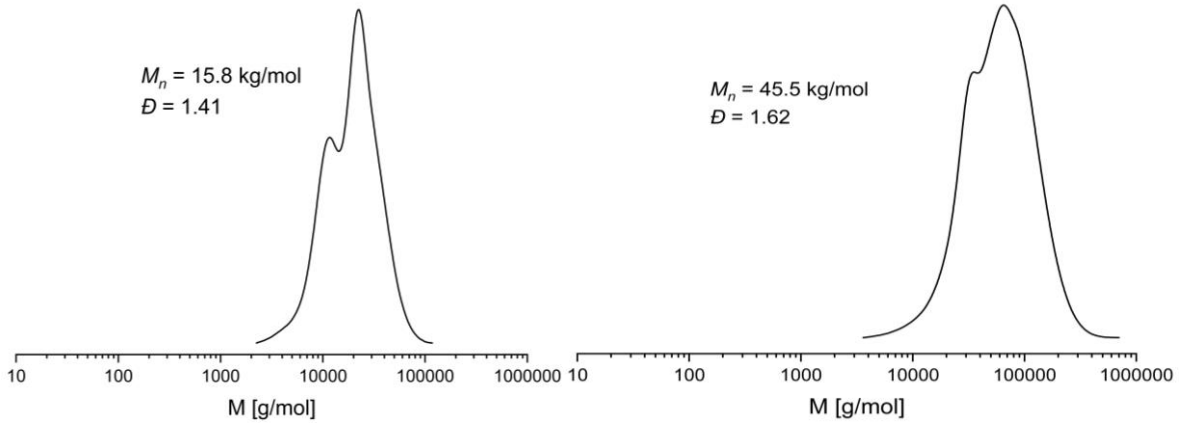

Table 2 run #1

Table 2 run #2

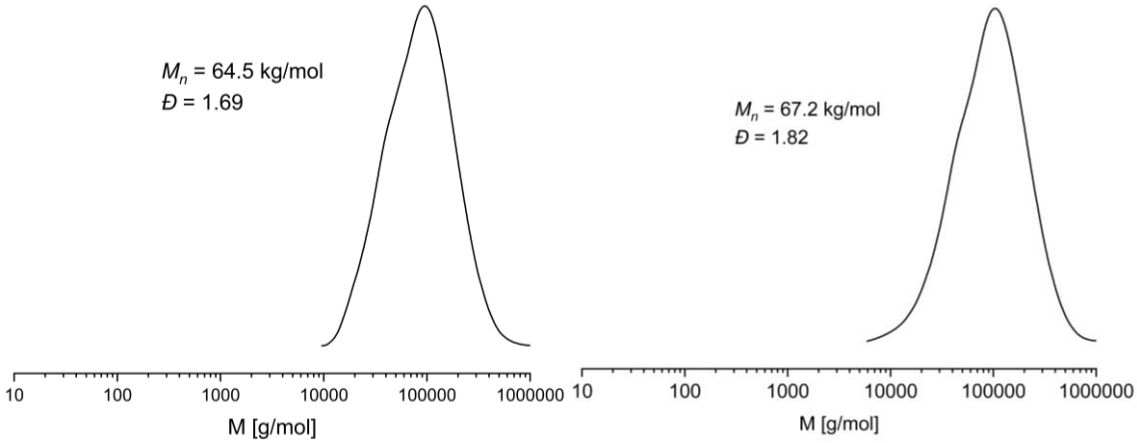

Table 2 run #3

Table 2 run#4

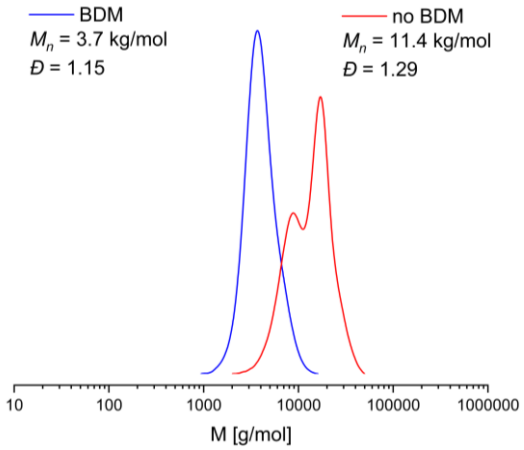

Figure S 43: GPC traces of PTA/vCHO copolymers corresponding to Table 2 as well as effects of the addition of 20 eq. of chain transfer agent (1,4- benzenedimethanol, BDM).

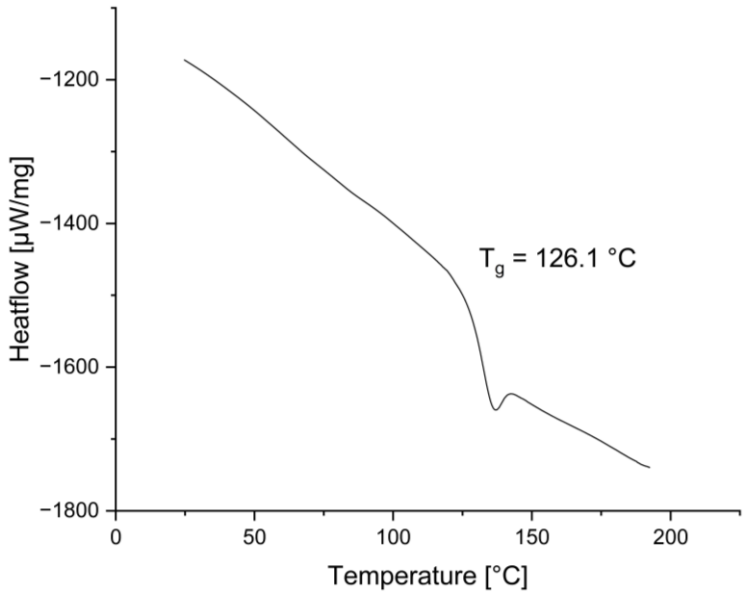

Figure S 44: DSC heating curve of the PTA/vCHO copolymer corresponding table 2, run #4.

Section S5: ROTERP with PTA/vCHO/CO_2

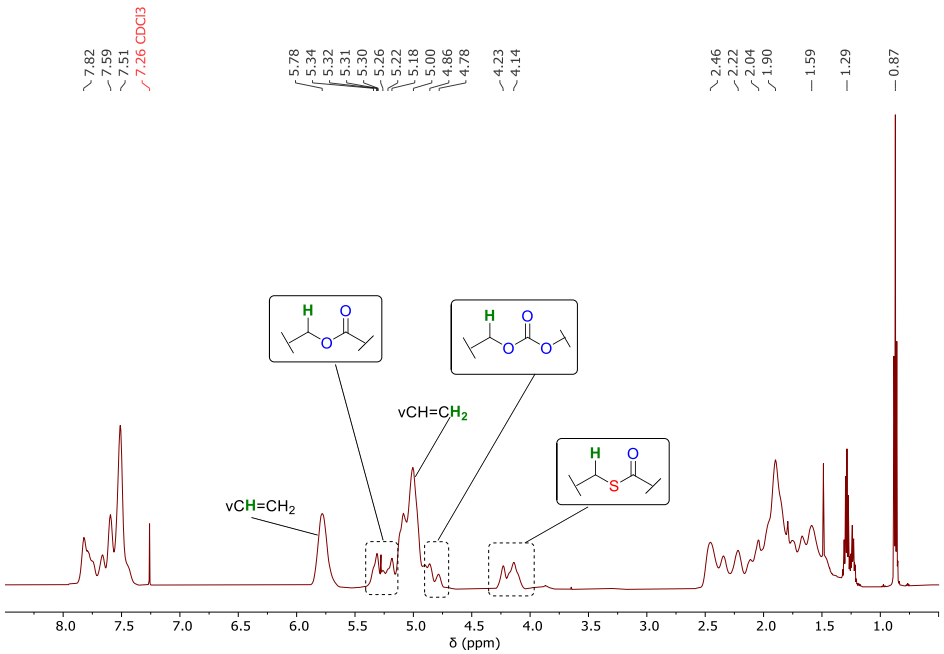

Figure S 45: ^{1}H NMR spectrum (400 MHz, $CDCl_3$) of isolated PTA/vCHO/CO_2 terpolymer from the run at 40 bar CO_2 pressure. Residual pentane from purification at 1.3 and 0.9 ppm.

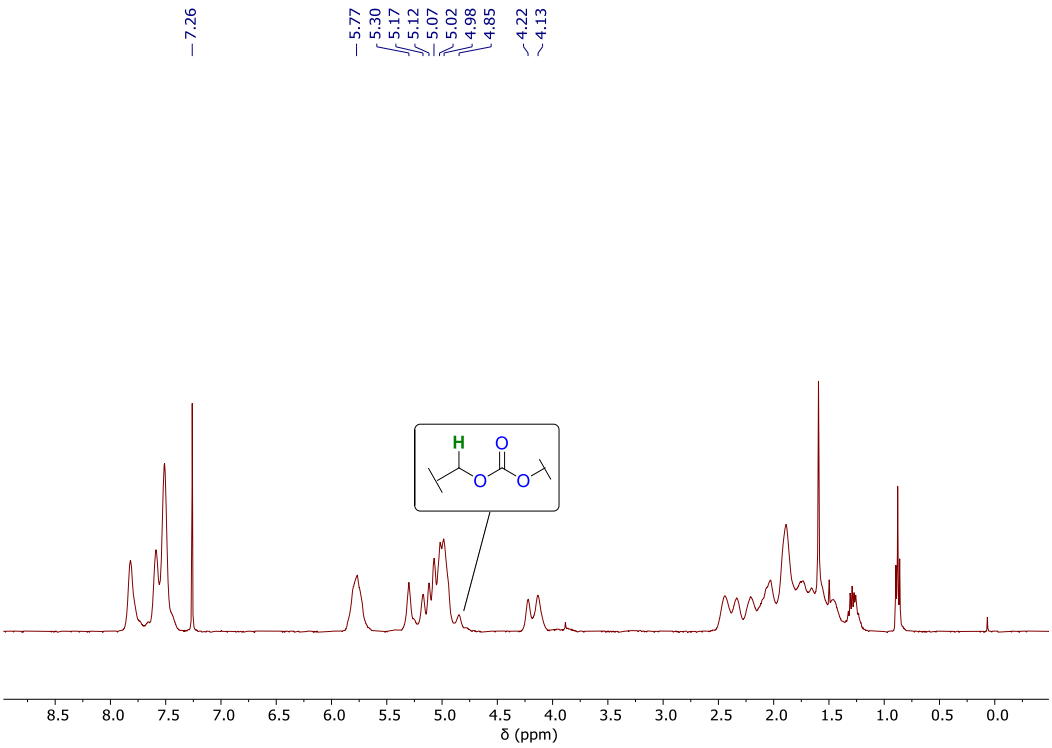

Figure S 46: ^{1}H NMR spectrum (400 MHz, $CDCl_3$) of isolated PTA/vCHO/CO_2 terpolymer from the run at 4 bar CO_2 pressure. Residual pentane from purification at 1.3 and 0.9 ppm.

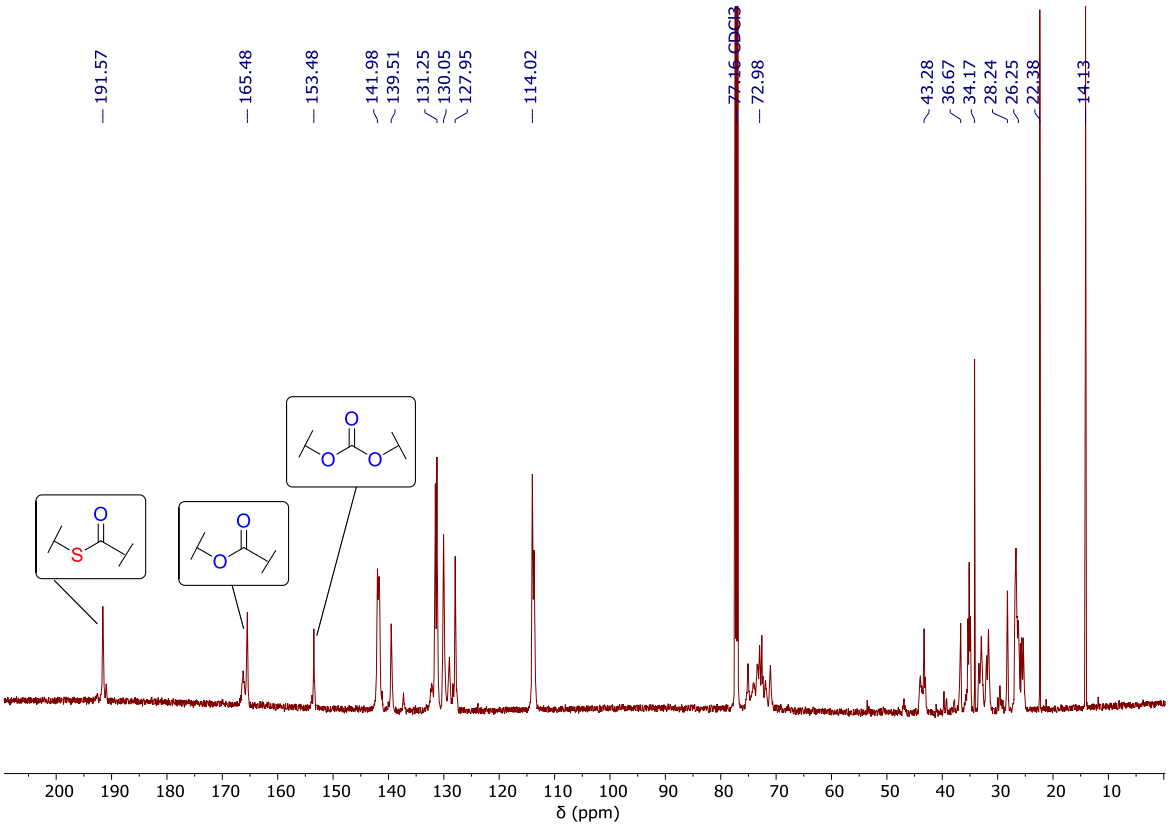

Figure S 47: ^{13}C NMR spectrum (126 MHz, $CDCl_3$) of isolated PTA/vCHO/CO_2 terpolymer from the run at 40 bar CO_2 pressure.

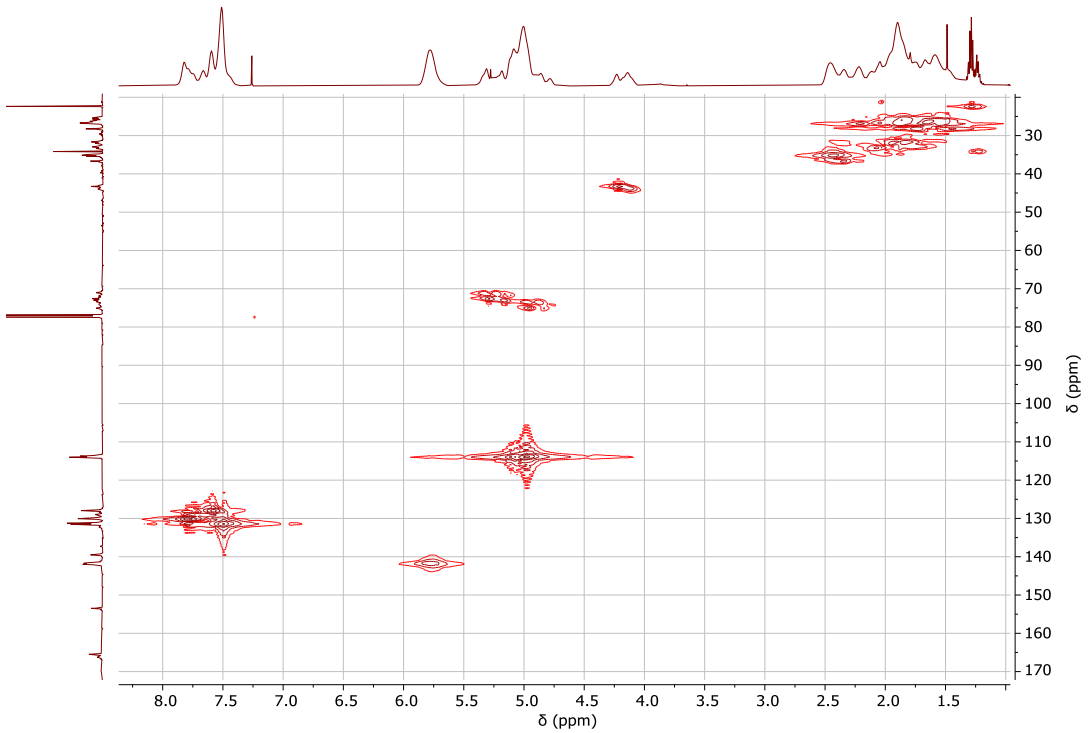

Figure S 48: ^{1}H - ^{13}C HMQC NMR spectrum (400MHz, $CDCl_3$) of isolated PTA/vCHO/CO_2 terpolymer from the run at 40 bar CO_2 pressure.

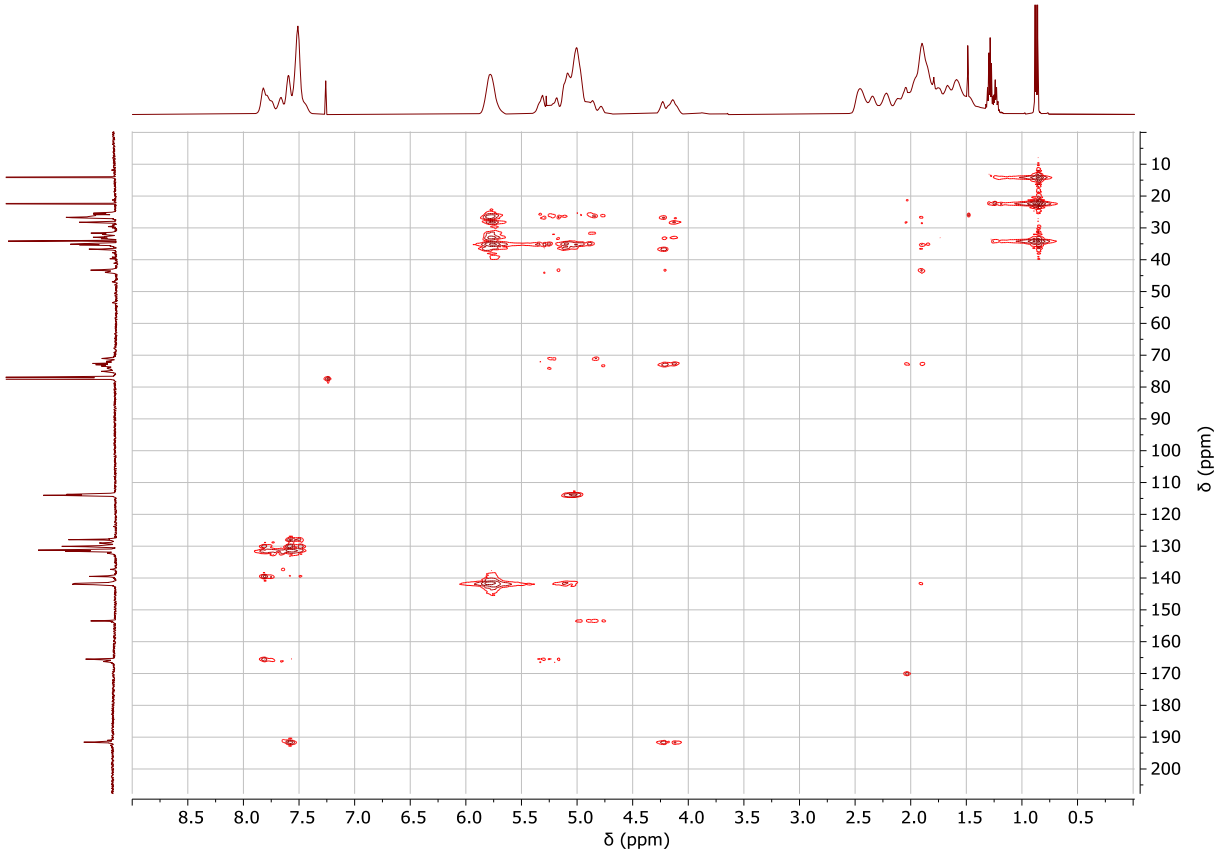

Figure S 49: ^{1}H - ^{13}C HMBC NMR spectrum (400MHz, $CDCl_3$) of isolated PTA/vCHO/CO_2 terpolymer from run at 40 bar CO_2 pressure.

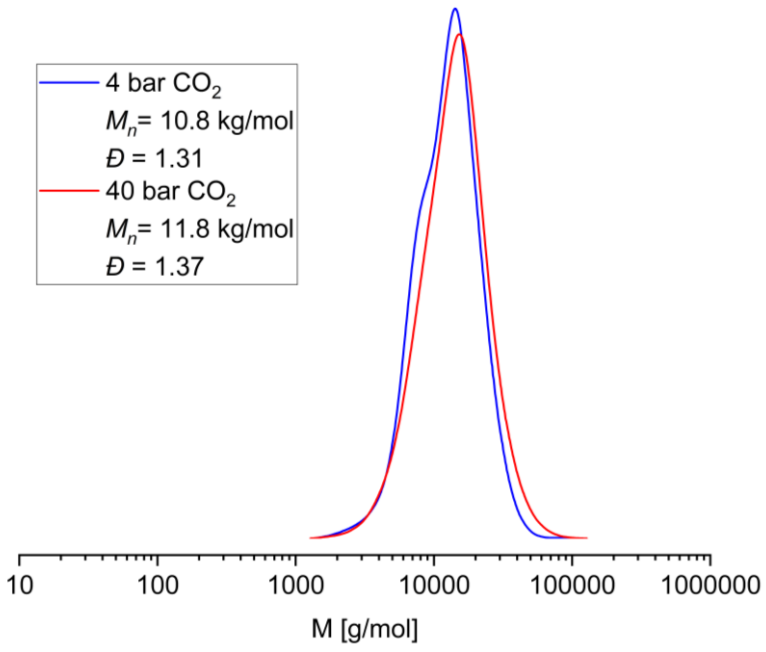

Figure S 50: GPC traces of PTA/vCHO/CO_2 terpolymers.

Section S6: Vinyl group functionalisation and degradation

Vulcanisation procedure: The PTA/vCHO copolymer from Table 2 run #4 was powdered and mixed with 10 wt% sulphur. Films were prepared by hot-pressing mixture between two aluminium plates covered with Teflon sheets heated between two LLG hotplates (held in place by a 5 kg weight on top) at 200 °C for 20 minutes. The vulcanized polymer film was obtained as a red, brittle sheet.

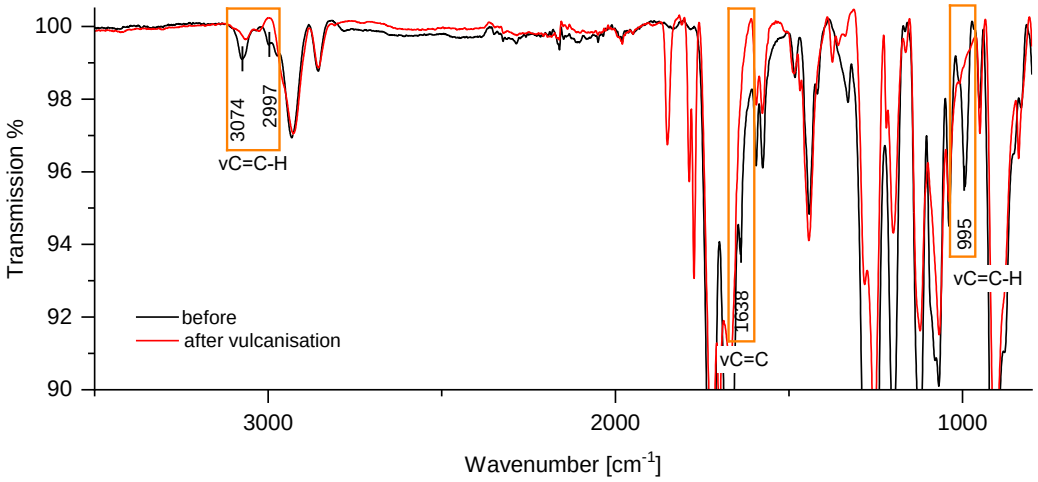

Figure S 51: FTIR spectrum before and after vulcanisation.

Aminolysis: The corresponding vulcanised polymer film (25 mg) was placed in 7 M ammonia in methanol (0.5 mL) in a 2 mL vial sealed with a melamine cap containing a Teflon inlay and equipped with a flame-dried magnetic stirrer for 1 week at room temperature.

Section S7: References

1 M. R. Stühler, C. Gallizioli, S. M. Rupf and A. J. Plajer, *Polym. Chem.*, 2023, **14**, 4848–4855.
2 E. J. K. Shellard, W. T. Diment, D. A. Resendiz-Lara, F. Fiorentini, G. L. Gregory and C. K. Williams, *ACS Catal.*, 2024, **14**, 1363–1374.